JOURNAL OF PROPULSION AND POWER
Vol. 19, No. 5, September–October 2003

Passive Control of Combustion Dynamics in Stationary Gas Turbines

Geo A. Richards* and Douglas L. Straub†
U.S. Department of Energy, Morgantown, West Virginia 26505
and
Edward H. Robey‡
Parsons Project Services, Morgantown, West Virginia 26505

This paper summarizes passive methods used to improve the stability of low-emission combustors in stationary power gas turbines. Common passive methods are reviewed, including discussion of control model concepts, application of simple time-lag models, and a review of acoustic dampers. Applications of time-lag modifications are presented, and limitations of this approach are discussed. Nyquist analysis is used to show how changing the time lag can be confounded by the presence of multiple acoustic modes. Experimental results demonstrating the frequency shifts predicted by Nyquist analysis are also shown. Stabilizing effects of distributed time lags are discussed, along with some field applications. A review of acoustic dampers shows that these devices are not widely applied in stationary engines compared to rocket or afterburner combustors, but have shown good results where applied.

Nomenclature*

AB, C, D, E, F, G	=	combustor sections and the acoustic transfer matrices that represent these sections; elements of these 2×2 matrices are identified using subscripts $A_{i,j}$ where $i = 0, 1$ and $j = 0, 1$
c	=	speed of sound, m/s
f	=	frequency, Hz
$\boldsymbol{G}$	=	transfer function relating relative heat release to relative acoustic pressure
$\boldsymbol{H}$	=	transfer function relating relative acoustic pressure to relative heat release
k	=	stagnation pressure loss coefficient
L	=	length, m
M	=	Mach number, μ/c
P	=	time-average pressure, Pa
p	=	complex acoustic pressure, Pa
Q	=	time-average heat-release rate, W
q'	=	complex amplitude of heat-release variation, W
R	=	acoustic transfer matrix for a cylindrical element
S	=	acoustic transfer matrix for a step expansion
s	=	cross-sectional area, m^2
T	=	gas temperature, K
Z	=	acoustic impedance, p/v, $(ms)^{-1}$
γ	=	ratio of specific heats
ζ	=	ratio of the speed of sound to area, c/s, ms^{-1}
μ	=	bulk gas velocity, m/s
v	=	acoustic mass velocity, kg/s
ρ	=	gas density, kg/m^3
τ	=	bulk time lag, s
ψ	=	transfer function relating acoustic pressure to velocity source, Pa*s/kg
ω	=	circular frequency, $2\pi f$, rad/s

*Applies only to Appendix

Received 4 October 2002; revision received 24 April 2003; accepted for publication 16 June 2003.

*Focus Area Leader, National Energy Technology Laboratory.
†Mechanical Engineer, National Energy Technology Laboratory.
‡Scientist.

I. Introduction

THIS special issue of the *Journal of Propulsion and Power* has highlighted the problem of achieving stable combustion in very low-emission gas turbines. As noted in the introduction of this issue, this problem has become a significant operational concern for low-emission engines now in service. Although engine developers and operators have indeed learned how to achieve stable combustion with very low emissions, this performance is often restricted to a tight operating window. These restrictions on the operating range lead to other issues, such as placing a cap on the peak power that can be produced,[1] more stringent requirements on fuel composition,[2] and routine "retuning" of the fuel splits.[3] These complications have been the motive to develop successful active control systems described elsewhere in this special issue. Active control offers the potential to readjust the combustion dynamics to accommodate problems like changing ambient conditions, fuel composition, or engine wear. Large-scale tests of active control, such as those reported by Seume et al.,[4] suggest that the active-control concept has significant potential, and might, in the future, be a preferred stabilization strategy. However, at the present time most engine developers are using passive methods to stabilize combustion.

This paper summarizes common passive methods used to improve the stability of low-emission combustors in stationary power gas turbines. In Sec. II, the discussion is aimed at helping the practicing combustion engineer gain familiarity with control model concepts that have become common in the literature. In Sec. III, the application of time-lag models for solving dynamics problems is discussed. This section also describes the similarities between the control concepts introduced in Sec. II and the time-lag models. Techniques to enhance stability, such as using multiple time lags or adding a pilot flame, are discussed. The nature of injector interactions are also described; this issue is often neglected in the research literature. In Sec. IV, a review of recent applications of acoustic dampers on stationary engines is presented.

II. Control System Models

Combustion dynamics are the result of an interaction between acoustic pressure p' and heat-release perturbations q'. This interaction can be described as a closed-loop feedback, shown schematically in Fig. 1. Acoustic pressure p' interacts with the flame and can produce a variation in the heat-release rate q'. The heat-release perturbation can in turn generate or amplify acoustic waves as described by Chu.[5] In a physically closed volume, such as a combustor,

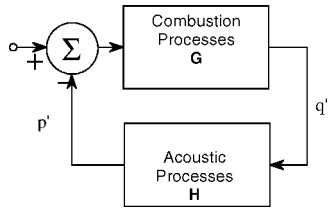

Fig. 1 Block diagram of a dynamic thermoacoustic system.

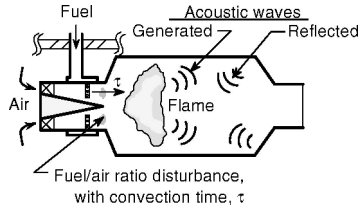

Fig. 2 Schematic of an unstable premixed combustion process.

the boundary conditions will establish standing waves, which can produce a periodic disturbance in the heat-release rate q'. The system will be unstable if the timing (phase) and the amplitude (gain) of these variations in pressure and heat-release rate produce constructive feedback. This feedback process is analogous to conventional feedback control systems, where the processes shown in Fig. 1 would correspond to control system components. The ***G*** and ***H*** nomenclature, as well as the summation circle follow directly from the control system literature and will be discussed in more detail later.

Because of the feedback analogy, control system models have become popular tools to both represent and diagnose combustion instabilities. Various levels of detail can be included in control system models, ranging from reduced-order models,[6] to computational fluid mechanics,[7] to complete engine models using a combination of approaches.[8] Practical application of these models has been demonstrated by many authors.[1,6,8–10] Even where a full model is not sought to solve a particular problem, it is helpful to understand the concepts because many experimental efforts to develop passive control can be explained by control system ideas. Thus, in what follows a simple representation of a control model for combustion dynamics is presented as a framework for subsequent discussions. Section II.A provides background so that no prior training in control theory is necessary and gives an example calculation to demonstrate the use of feedback models. Section II.B reviews the physical processes that contribute to the flame response. Section II.C reviews predictions of the flame response and various approaches to predict combustion system stability.

A. Stability Analysis of an Example Problem

A schematic of a typical fuel–air premixer and combustor is shown in Fig. 2. Acoustic waves are generated at the flame by variations in heat-release rate q'. The creation of sound by unsteady heat release is a complex process,[5] but in simple terms q' perturbations create expansion and contraction of the gas, generating pressure waves. These pressure waves are reflected and continue to interact with the flame such that standing waves are established in the combustor. In Fig. 1 the feedback element (***H***) represents the conversion of heat-release variations into a pressure disturbance. If the heat release could be manipulated at a periodic rate, the output signal from Block H would represent the pressure produced in the flame region. This pressure has contributions from sound generated at the flame and from the standing wave established by reflections from the combustion liner. For oscillating frequencies that typically occur in gas turbine engines, the wavelength is usually long enough that the entire flame can be treated as if a single pressure perturbation is acting on it.

In Fig. 1 the system element (***G***) represents the conversion of a pressure variation to a variation in the heat-release rate. Many mechanisms can contribute to a variable heat-release rate. These mechanisms can include periodic changes in the flame surface area,[11] changes in equivalence ratio,[1,12–17] vortex shedding,[18–23] changes in the bulk flow,[24] and changes in flame anchoring.[25–27] Which of these mechanisms contribute to oscillations in a given problem is an important practical question and is discussed in Sec. II.B. However, attention is often focused on the equivalence ratio variation because it will usually accompany all of the other mechanisms. The pressure drop across the premixer air passage is typically a few percent of the operating pressure. Modest perturbations in the combustor pressure will thus create significant variations in premixer airflow and fuel–air ratio in the premixer. Fuel–air perturbations are then transported to the flame after a convection time lag τ, creating a heat-release perturbation that can add to perturbations produced by other mechanisms, such as a variable flame area.

If attention is restricted to small perturbations about the mean conditions, linear stability can be assessed. To perform this analysis, the transfer functions depicted in Fig. 1 must be known in sufficient detail. The next few paragraphs review the basic ideas connected with transfer functions so that the subsequent discussion can be understood without prior knowledge of automatic control theory.

Figure 3a shows a schematic of a transfer function. An input signal $A\cos(\omega t)$ enters at the left, and a resulting signal $B\cos(\omega t+\phi)$ exits at the right. Considering a range of frequencies ω, the ratio B/A is the gain of the transfer function, and ϕ is the phase angle. It is algebraically simpler to consider the complex counterpart to these real quantities (see Fig. 3). In that case the input and output are $Ae^{j\omega t}$ and $Be^{j(\omega t+\phi)}$. Using this notation, the constant B can redefined as a complex quantity including the phase angle ($B'=Be^{j\phi}$), so that the transfer function simply relates complex quantities A to B'. In this manner the time dependence is not needed in a feedback loop analysis because all the blocks have the same time dependence $e^{j\omega t}$. Thus, the transfer function is the complex ratio of the output to the input or B'/A.

Sequential processes, where the output of one transfer function supplies the input to a second process, are analyzed by multiplying the transfer functions in order. As shown in Fig. 3b, if the B'/A process just described connects to a D'/C process the net transfer function is $(B'/A)*(D'/C)$. Signals can also be added algebraically because attention is restricted to linear systems. For example, a given input can supply both the A-B' transfer function and the C-D' transfer function, with the outputs combined (Fig. 3c). The combined gain and phase are the complex sum $(B'/A)+(D'/C)$. By adding or multiplying individual transfer functions, it is possible to combine the various "blocks" that represent physical processes

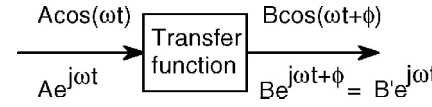

a) Transfer function nomenclature

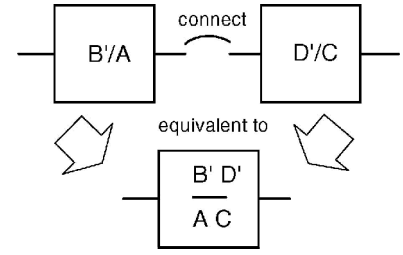

b) Series connection of transfer functions

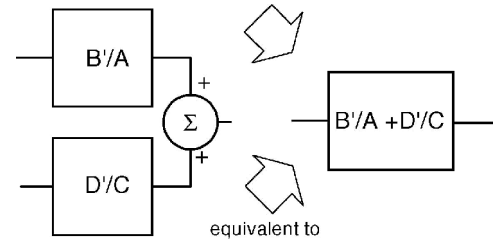

c) Parallel connection of transfer functions

Fig. 3 Illustration of transfer function nomenclature and block diagram manipulations.

to just the forward transfer function (usually denoted $\boldsymbol{G}$) and the feedback transfer function (usually denoted $\boldsymbol{H}$).

For a combustion problem once the various processes have been described and the problem is reduced to the form shown in Fig. 1, the response of the system to disturbances can be considered. As shown in Fig. 1, a disturbance is added to the signal at the summing point. In this paper the feedback that emerges from $\boldsymbol{H}$ is subtracted from the disturbance. (In the control theory literature this is known as "negative feedback." Physical processes represented in block $\boldsymbol{H}$ are multiplied by -1 to produce the negative feedback.) With this nomenclature disturbances that originate at the summing point will pass through $\boldsymbol{G}$ and $\boldsymbol{H}$, with modifications to both amplitude and phase. Note that a phase of 180 deg (π) corresponds to multiplication by -1 [i.e., $\cos(\pi)$]. Intuitively, if the disturbance is returned from H with a larger absolute magnitude and a negative sign it will pass through the negative branch of the summing point, multiplying by another -1. Therefore, the original disturbance will have a larger amplitude after passing through $\boldsymbol{G}$, $\boldsymbol{H}$, and the summing point. Under this idealized condition the disturbance will lead to an instability because it will grow in amplitude each time it passes around the loop.

This intuitive understanding can be matched by formal analysis that leads to a criterion for stability. The output of a signal passed through $\boldsymbol{G}$ and $\boldsymbol{H}$, but not returned through the summation point, is known as the open-loop frequency response. The open-loop frequency response can be used to evaluate stability from both Bode and Nyquist plots described next.

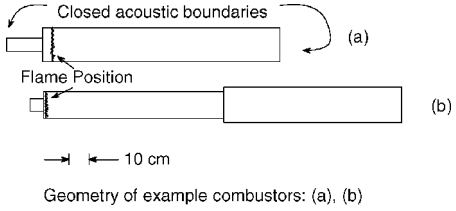

Fig. 4 Schematic of combustor geometries used in the example problems.

The open-loop response of some simple transfer functions will now be considered. Two combustor examples shown in Figs. 4a and 4b will be analyzed. The fuel–air premixer at the left supplies a step expansion into the region where the flame is stabilized. The flame is treated as a disk located just downstream of the step expansion. The remainder of the combustor is a long tube, including a second step expansion in Fig. 4b, and then terminated at a closed acoustic boundary. These examples approximate the conditions typically encountered in combustion test rigs, where the downstream boundary can represent a backpressure control valve. For the calculated results presented next, parameters such as pressure, temperature, flow rate, and fuel–air ratio are all selected to be representative of gas turbine combustors.

Treating the flame as a discontinuity that interacts with acoustic waves, a one-dimensional acoustic analysis is used to determine the acoustic pressure produced by imposed heat-release perturbations. For the geometry shown, this is accomplished using the flame-acoustic relations presented by Chu[5] and analyzing the acoustics with the transfer matrix method.[28] An outline of these calculations is presented in the Appendix. The transfer matrix method can be easily applied to this type of problem and can account for mean flow effects and acoustic losses at abrupt area changes. Let P and Q represent the steady-state values of pressure and heat-release rate in the combustor. Using the methods shown in the Appendix, the normalized pressure response (p'/P) to a normalized heat-release perturbation (q'/Q) is shown in Fig. 5a. These results correspond to the combustor geometry in Fig. 4a. The plot shows that the acoustics of the system produce a strong response to heat-release perturbations at ~240 Hz. This maximum amplitude corresponds to the natural frequency of the system. Figure 5a also indicates that the system has a pressure node near the flame at ~140 Hz. At this frequency there is no pressure response at the flame to perturbations in the heat-release rate. Near 140 Hz the phase abruptly changes from

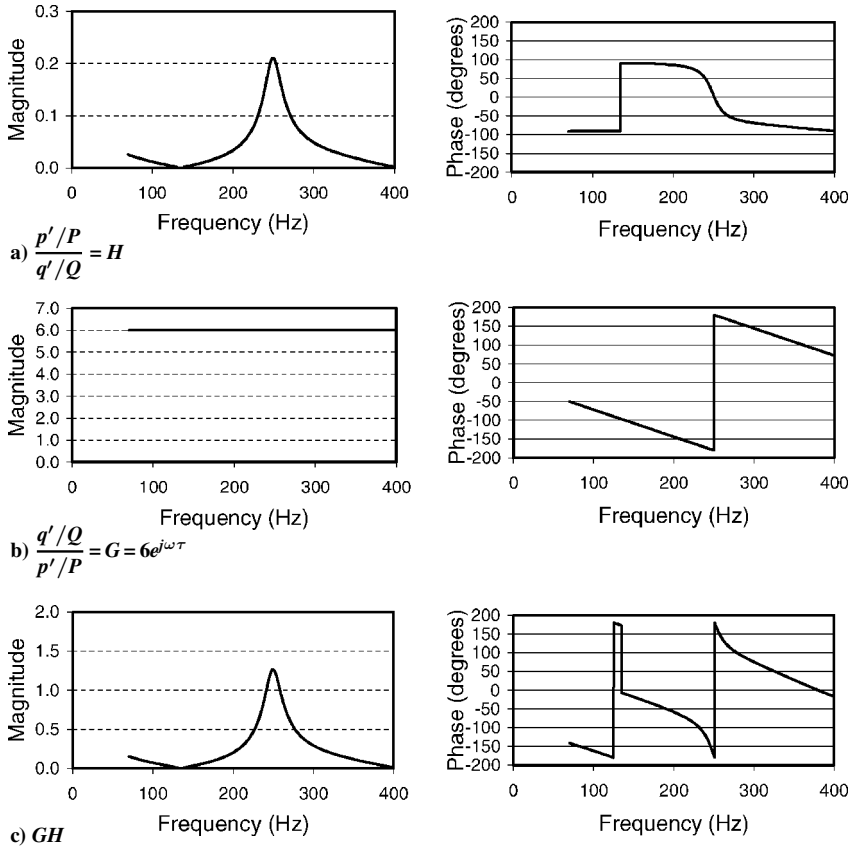

Fig. 5 Frequency response (Bode plots) of transfer functions used in the first example problem with a single acoustic mode (Fig. 4a).

−90 to +90 deg; this is expected behavior for acoustic nodes. As the frequency approaches 240 Hz, the phase begins to drop off as the amplitude rises, with another transition from +90 to −90 deg. This is typical of a resonant frequency. The magnitude of the amplitude peak and the width of the phase transition (phase roll) are both related to the acoustic losses in the system. Here, acoustic losses arise from the step expansion, mean flow, and mean heat release. For this example Fig. 5a represents the ***H*** transfer function depicted in Fig. 1.

The combustion response to acoustic pressure perturbation must also be analyzed. In actual applications this response must account for the various mechanisms described earlier: variable fuel–air ratio, variable flame area, etc. These various response mechanisms are described later in Sec. II.B. For the purposes of illustration, a simple transfer function will be considered. Again referring to the normalized perturbations (p'/P and q'/Q), the flame will be treated as having a constant gain of magnitude 6.0, but with a time delay $\tau = 2$ ms relative to the acoustic pressure at the flame. This transfer function is $6.0e^{-j2\pi\tau f}$. Thus, a normalized pressure perturbation produces a normalized heat-release rate perturbation six times larger and 2 ms later, which is easily realized in practical systems. This transfer function is shown in Fig. 5b. The phase plot in Fig. 5b is representative of all time-delay systems. The phase angle decreases in a linear fashion with frequency because the phase angle $\theta = -2\pi\tau f$. In this plot the phase angle is "wrapped" into the range −180 to +180 deg. The same information can be plotted from 0 to 360 deg as well, avoiding the abrupt discontinuity at ±180 deg.

The open-loop response of this example is the series connection of both the ***G*** and ***H*** transfer functions. As just explained (Fig. 3), this series connection is computed as the product of the individual gain functions, and the phase angles are added. The resulting frequency response is shown in Fig. 5c. Note that the magnitude is greater than unity at ∼240 Hz, and the phase angle is ±180 deg. If this ***GH*** output is connected to the summation point in Fig. 1 (i.e., closed loop), the system would be unstable for the reason explained earlier: the returning signal would grow in amplitude each time around the loop. If the gain were less than 1 at a phase angle of ±180 deg, the system would be stable because returning signals would decrease in amplitude each time around the loop. This reasoning is not entirely complete; there are more complications if the magnitude plot crosses magnitude 1.0 more than once. This complication is accounted for using a Nyquist analysis, discussed next. The presentation that follows is an adaptation of analysis discussed by Fannin et al.[29]

A complete description of Nyquist analysis is found in control textbooks (see Phillips and Harbor[30]). A brief description is provided here to demonstrate the value of Nyquist analysis, but it is not intended to be a complete tutorial. The Nyquist analysis requires plotting the same information as in the Bode plots, but in polar form. In polar form the radius is equal to the magnitude, plotted at an angle equal to the phase angle. For example, magnitude 1.0, at 0 deg of phase is point $(1, 0j)$ on the positive, real x axis. Magnitude 1.0 at 90 deg of phase is the the point $(0, 1j)$ on the positive imaginary axis, and so on. Figure 6 shows Nyquist plots for the example problem presented in Fig. 5 at three different values of the time lag. The center plot in Fig. 6 shows a Nyquist diagram corresponding to Fig. 5c, where the time lag is 2 ms. The circular lobe corresponds to frequencies between 200 and 300 Hz, where there is appreciable magnitude from the open-loop response. For clarity, three of the frequencies are indicated on the lobe; the corresponding points (phase, magnitude, and frequency) can be found from a close inspection of the Bode plot in Fig. 5c. Note that the lobe represents a very small range of frequencies in this example problem.

As explained in control theory textbooks, the system stability can be evaluated by counting how many times the Nyquist plot "encircles" the point −1 on the x axis. The definition of what constitutes encirclement is fairly involved, and one must refer to control textbooks for complete details.[30] In brief, encirclement direction (clockwise or counterclockwise) must be counted as positive or negative encirclement, and the sum of all of the positive and negative encirclements are added to arrive at a net number of encirclements. The plot also requires considering information at negative frequencies—essentially a reflection of the Bode plot into the negative frequency axis. And, the open-loop system must itself be stable. In this example problem these details do not enter the discussion, but should be considered before using Nyquist analysis on more complex problems. The complete Nyquist analysis predicts that the system will be unstable if the net number of encirclements is greater than zero. Figure 6b shows that the Nyquist plot does indeed encircle −1 on the real axis and would therefore be unstable.

The benefit of the Nyquist analysis becomes very apparent when assessing how different time lags affect system stability. Figure 6 shows the open-loop system ***GH*** at three different values of the time lag: $\tau = 1.6$, 2.0, and 2.6 ms. Increasing the time lag rotates the lobe clockwise. This behavior can be understood by noting that over the small frequency range where the amplitude is significant (230–270 Hz) changes to the phase angle $\theta = -2\pi\tau f$ are dominated by changes in τ. Changes in τ appear to rotate each point on the lobe approximately the same angle, producing a rotation of the lobe.

The Nyquist plots can also be used to investigate stability boundaries for the system. For example, both the short and the long time lags shown in Fig. 6 almost encircle the −1 point on the real axis. The values of τ that almost produce encirclement of the −1 point are stability boundaries for the system. Each of these stability boundaries, or values of τ, have a corresponding frequency at which the lobe crosses the negative real axis. In this example the system would be unstable for frequencies of 258 and 241 Hz at $\tau = 1.6$ and 2.6 ms, respectively. The frequency range and the size of the lobe in the Nyquist plot depend on the roll off in the phase angle function. For problems that have larger acoustic losses, the phase roll off near the resonant frequency can cover a larger frequency range, and the lobe in the Nyquist plot would also cover a wider range of frequencies.

If the system in this example were actually operated in the closed-loop mode, the limit-cycle frequencies could be estimated from the so-called describing function theory.[30] Under the assumption of real-valued describing functions, the limit-cycle frequency would correspond to the frequency at which the Nyquist plot crosses the negative real axis. Considering the sequence of time lags in Fig. 6, the implication is that as the time lag increases from 1.6 to 2.6 ms the frequency would change from 258 to 241 Hz. This frequency shift as a function of time lag is a general feature of the Nyquist analysis, and the range of frequencies depends on the specific case, as just noted. An experimental example of the frequency shift will be shown in Sec. III.A.

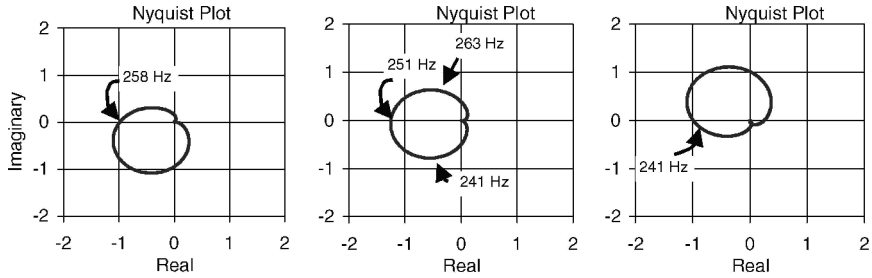

a) $\tau = 1.6$ ms **b) $\tau = 2$ ms** **c) $\tau = 2.6$ ms**

Fig. 6 Nyquist plots for the single acoustic mode example (Fig. 4a) at three different time lags.

In Figs. 5 and 6 the combustor acoustic response has been characterized by a single acoustic mode. [Higher-order modes could also be considered in a simple geometry like Fig. 4a. The Bode plot (Fig. 5a) frequency range could be extended to higher frequencies to account for these harmonics, and the analysis would be unchanged.] The second example geometry shown in Fig. 4b is slightly longer and has an additional step expansion. Calculations for Fig. 4b are now conducted in exactly the same manner as in the preceding example. However, the combustion gain is now reduced from 6.0 to 1.0 for convenience. Therefore, the $\boldsymbol{G}$ portion of the transfer function is simply $e^{-j2\pi\tau f}$. The resulting Bode plot with $\tau = 1.5$ ms is shown in Fig. 7. This second example has strong acoustic responses near 185 and 410 Hz. Note that the magnitude plot is greater than unity at both of these resonant frequencies, and so it is more difficult to visualize the stability limits based on the Bode plot alone. This is a case where the Nyquist analysis is much easier to use. Figure 8 shows the Nyquist analysis for three different values of the time lag. As before, increasing the time lag has the effect of rotating the lobes clockwise. Starting at $\tau = 0.9$ ms, the system is stable, but near a high-frequency stability boundary (411 Hz) the -1 point on the real axis is almost encircled. Increasing the time lag to $\tau = 1.5$ ms makes the system unstable to the high-frequency mode (408 Hz). Note the high-frequency lobe encircles the -1 point on the real axis, but the low-frequency mode does not. A further increase to $\tau = 2.0$ ms causes the instability to shift frequency modes and become unstable at 184 Hz.

The rotation of these lobes underscores the fundamental problem with achieving stability from changes to the combustion time lag, that is, by changing the phase. Changes in time lag can simply change the oscillating frequency rather than produce stability. Even when a combustor has just a single dominant acoustic mode, the width of the phase roll can produce oscillations over a range of frequencies corresponding to the range of selected time lags as shown in Fig. 6. In summary, careful consideration must be given to the acoustic modes before attempting to solve a dynamics problem by adjusting the time lag.

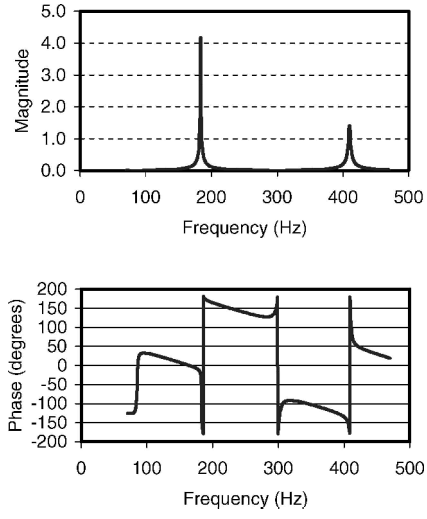

Fig. 7 Open-loop frequency response (Bode plot) for the example with two resonant acoustic modes (Fig. 4b, $\tau = 1.5$ ms).

The preceding example assumed that the flame response is a constant magnitude. In real applications the transfer function magnitude and phase are governed by the flame response to acoustic perturbations. As just noted, this response can involve multiple physical processes that are often difficult to differentiate. Section II.B reviews the physical processes associated with the flame response and various approaches to use them in a transfer function description.

B. Physical Processes Contributing to the Combustion Transfer Function

The heat release from a premixed flame is the product of the reactants consumed by the flame times the heat of reaction and can be written as

$$Q = \rho Y_f S A_f \Delta H \tag{1}$$

where Y_f is the mass fraction of fuel in the premixed gases, S is the flame speed, A_f is the area of the flame, and ΔH is the heat of reaction per unit mass of fuel. Based on this equation, it is clear that the heat release can vary with perturbations in density, fuel mass fraction, flame speed, and flame area. In gas turbine combustion the density perturbations arising from acoustic pressure are typically much smaller than the other terms and are often neglected. Oscillating aerodynamics can produce a significant modulation in flame area and should not be neglected. Likewise, changes in the flow of either fuel or air will change the fuel mass fraction and the flame speed. In what follows, consideration is first given to transfer functions of fully premixed flames, with constant fuel/air ratio, before considering the combined problem of fuel/air variation and flame-area response.

The transfer function of fully premixed flames has been investigated by various authors. Blackshear[31] proposed one of the earliest models for the response of a premixed burner to acoustic perturbations. Applying mass and momentum conservation around a control volume that enclosed the flame, this author showed that variations in the flame area were responsible for the driving or damping acoustic waves imposed on the burner. Companion experiments demonstrated that damping of the flame depended significantly on the mean flow velocity and the fuel-air ratio. Merk[32] presented an improved analysis of a premixed burner flame and was able to derive an explicit expression for the flame transfer function. The transfer function is a first-order response (i.e., the solution of a first-order ordinary differential equation.) for the dimensionless flame-area fluctuation A' produced by a perturbation in the dimensionless supply velocity u':

$$A' = \frac{1}{1 + j\omega\tau_1} u' \tag{2}$$

Here, the perturbation quantities are normalized by their corresponding steady-state values. The analysis identifies a characteristic time τ_1 that represents the average time for gas exiting the burner to be consumed by the flame cone. For clarity, the notation τ_1 is used to make a distinction with the convective time-lag τ identified in Fig. 2, which includes the premixing process. At large values of $\omega\tau_1$, Eq. (2) predicts that the flame-area response magnitude will be much less than one and approach a phase of -90 deg. This is different than the pure time-lag response $e^{j\omega\tau}$ described earlier, which will have

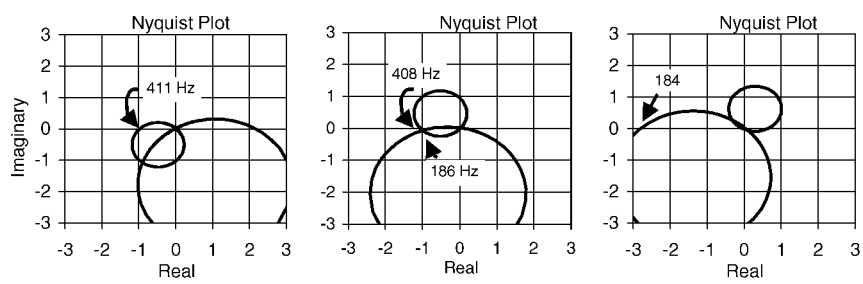

a) $\tau = 0.9$ ms **b) $\tau = 1.5$ ms** **c) $\tau = 2.0$ ms**

Fig. 8 Nyquist plots for the example with two resonant acoustic modes (Fig. 4b) at three different time lags.

arbitrarily large phase angles for large $\omega\tau$. This distinction will be noted in a comparison to experiments discussed later. Using Eq. (2) and an acoustic analysis, Merk[32] showed that stable and oscillating combustion could be produced by selected ranges of the time lag. Merk[32] did not include any experimental results, but noted that the predicted transfer function depended on the flame speed (and thus the fuel-air ratio) and the mean flow velocity in the same manner as shown experimentally by Blackshear.[31]

Further investigations of the flame transfer function have been carried out by a number of authors, including both analytic work and experimental data.[11,33–37] Becker and Gunther[33] investigated a premixed turbulent jet flame with excitation driven by an oscillating exhaust valve. Results were limited to relatively low frequencies (<30 Hz), and the expression for the transfer function was fit to the experimental data by suitable choice of a time lag. Mugridge[35] predicted the stability of a multi-port premixed burner, based on the model proposed by Merk.[32] The burner arrangement was intended to mimic the model, but predictions of stable and oscillating combustion did not correspond to measurements. The author concluded that more work was needed to predict the flame transfer function. For this reason Mugridge[35] also reports preliminary attempts to measure the transfer function, using techniques described by Hadvig.[38] Although few experimental details are given, the measured transfer function showed considerable variation in the phase of the response over relatively small frequency ranges, in contrast to model expectations.

Matsui[36] investigated experimental data from three multiport premixed burner configurations and again identified a characteristic time lag in the flame transfer function. Matsui compared the various transfer functions that had been published to that time and noted that the magnitudes were similar, but their phases angles were considerably different. Matsui's transfer function includes a multiplier with a pure time lag term ($e^{j\omega\tau}$). As just noted above, the transfer function phase angle could therefore reach arbitrarily large phase angles for large $\omega\tau$.

More recently, Fleifil et al.[11] developed an analytic model for the flame transfer function, which describes the distortion of the flame surface area in response to imposed velocity perturbations at the base of the flame. Unlike earlier work,[31,32,36] this model accounted for the distortion of the flame surface by tracking the kinematics of the flame movement in the oscillating flow. The variation in heat release again results from the variable flame surface area. The predicted transfer function is qualitatively similar to earlier models and can be approximated as a first-order system, that is, Eq. (2). No experimental data were used to verify the predictions.

Using a very similar theoretical model as Fleifil et al.,[11] Ducruix et al.[37] compared the measured and predicted flame transfer function of a bunsen flame with an oscillating supply of premixed gases. Laser Doppler Velocimetry was used to directly measure the oscillating velocity at the base of the flame, and global CH* chemiluminescence was used to indicate the oscillating heat release. The input flow was excited by a loudspeaker in the supply plenum at frequencies up to ~200 Hz. In this manner, a direct measure of the transfer function between the oscillating velocity and heat release was obtained. Compared to the theoretical model, the magnitude of the transfer function was predicted reasonably well for two different burner configurations and at several operating conditions. In contrast, the phase of the transfer function was poorly predicted for frequencies beyond ~30 Hz. Above this frequency the phase of the response depended significantly on the mean flow velocity and the burner dimensions. The (negative) phase exceeded −360 deg, in contrast to the theoretical model, which was limited to −90 deg, as in Eq. (2). The authors suggest that the discrepancy is caused by the model assumption of uniform axial flow at the base of the flame. Experiments (not reported) showed that the spatial velocity distribution at the base of the flame must be accounted for to improve model predictions.

The preceding discussion emphasizes the uncertainties connected with predicting a flame transfer function, even for relatively simple premixed bunsen or jet flames. In bluff or step-stabilized flames, such as those used in afterburners, or dump combustors, flame-area variations can originate from oscillations in the size of the shear layer and from vortex merging.[18–24,39] In swirl-stabilized flames these aerodynamic phenomenon are even more complicated. The swirl angle, the size of the combustor step expansion, and the length of the combustor can all affect the flow dynamics. Thus, for swirl flames there is no general approach to estimate the contribution of the flame-area variation to the flame response. Some recent papers reporting measured or predicted transfer functions for swirl flames are discussed later.

In addition to aerodynamic processes, the oscillating heat release in turbine combustors will be simultaneously influenced by changes in the fuel/air ratio. Oscillating pressure in the combustor will produce a dynamic response of the premixed air, fuel, or both, creating a variable heat release when the mixture arrives at the flame. As already noted in Fig. 2, mixture perturbations formed in the premixer are convected to the flame after a time lag τ. These fuel/air variations are not formally part of a flame transfer function because they are produced by the supply system that feeds the flame. Nevertheless, it is convenient to describe the combustion response including the system dynamics and refer to this as the transfer function for combustion. Various analyses of the feed system dynamics are available in the literature for rockets, industrial burners, and gas turbines.[1,14,40–44] Several recent papers consider the effect of the mixing processes during fuel injection[45,46] and suggest that it is necessary to account for the dispersion of fuel/air perturbations in the premixer when assessing the overall combustion response. Mongia et al.[17,47] demonstrate a simple absorption technique to measure the fuel/air fluctuations that occur during premixed combustion oscillations. Lee et al.[16] combined the measurement of the fuel/air oscillations with a measurement of the total heat-release oscillation and showed that the fuel/air variation was the primary contribution to the oscillating heat release, at least for their test configuration.

Perracchio and Proscia[6] extend the model of Fleifil et al.[11] to include both the variation in flame area and the simultaneous variation in fuel/air ratio. With an appropriate choice of empirical parameters, this approach produced a useful model of the heat-release response to acoustic perturbations, and the predictions compared favorably with measurements of the heat release. Based on visual observations of the flame and computational fluid dynamics not reported, the authors comment that the role of flame-area variations is very significant and probably larger than expected from a simple flame model. This is in contrast to other experiments[48] that show only modest structural change in practical turbine flames during oscillations. This is not a general result; the same combustor exhibited significant flame-area variation when tested at atmospheric pressure.[48] In other testing Kendrick et al.[26] specifically mention that "the unsteady combustion process appears to be controlled by periodically shed toroidal vortex structure. . . ." Thus, it can be stated that the contribution of flame area vs fuel/air ratio to the flame transfer function is very dependent upon the specific situation. Kendrick et al.[26] compared the dynamics of two different fuel/air premixers and showed that flame anchoring methods will significantly affect the flame response. One premixer used aerodynamic stabilization of the center recirculation zone, and the second premixer used a bluff-body stabilization (with swirl). The aerodynamic stabilization was noted to provide weaker flame anchoring, allowing the flame reaction zone to oscillate axially in the flow throughout the pressure cycle. This axial movement can add another complexity to the flame transfer function. Schuermans and Polifke[25] note that it is necessary to include flame translation in their analytic model of the flame response.

A number of recent papers have attempted to measure the dynamic response of premixed, swirl-stabilized flames that are characteristic of low-emission gas turbines.[49–53] Paschereit et al.[49] demonstrate an acoustic technique to measure the transfer matrix of a premixed gas turbine burner. This matrix can be used in a stability analysis similar to the transfer function. Lawn[50] measured the phase of the acoustic velocity "jump" across a swirl-stabilized laboratory flame. With some empirical adjustment to a corresponding analysis, the author was able to explain observed frequency selection in the burner. Krebs et al.[51] directly measured the transfer function of a gas turbine fuel nozzle. The supply of fuel and air was modulated to produce a forced oscillation, with the response of the heat release measured by flame

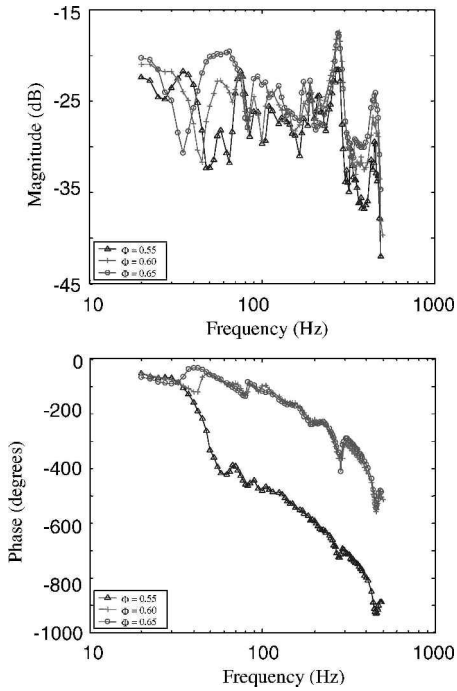

Fig. 9 Measured flame response at to perturbations in acoustic velocity equivalence ratios Φ from Khanna.[52]

chemiluminescence. The measured response is described by a time-lag model, but the measured time lags are larger than predicted from a computational fluid dynamics model. Khanna[52] and Khanna et al.[53] also measured the flame transfer function of a swirl-stabilized flame. An example of the flame transfer function is shown in Fig. 9. This is the flame heat-release response to acoustic velocity perturbations in the fuel/air premixer. These data correspond to a swirl-stabilized flame, with fuel-air premixing similar to what is used in gas turbine applications. Data are shown for three different equivalence ratios. Note that the magnitude curve is very complicated, having several peaks and minima. The authors suggest that part of the response is associated with near-field acoustics that are not accounted for in a simple feedback model between the local acoustic pressure p' and the heat release. The large values for the phase angle and the drop with frequency are indicative of a time-lag response, which is noted in a corresponding analysis.[52,53] The phase plot also demonstrates a significant change in the phase with equivalence ratio. Note that the change from $\Phi = 0.6$ to 0.55 produces an abrupt change in the phase. This remarkable change would have the effect of changing the orientation of the lobes in the Nyquist plots discussed earlier and is an example of how the flame dynamics can change appreciably with relatively minor changes in operating conditions.

C. Prediction of Transfer Functions and Combustion System Stability

A number of investigations have used computational fluid dynamics (CFD) to predict the flame response.[7,8,54–58] Because CFD solutions converge in the time domain, the results must be transformed into the frequency domain for use in a stability analysis. Some authors[8,55,56] have used CFD to model the response of a flame to a step change in the reactant flow. A Fourier transform of the response then provides the desired frequency-domain flame response. Compared to limited experimental data, the approach requires some empirical filtering to produce reasonable agreement with experiments.[56] The same technique was extended to include the frequency response of a burner supply system by Kruger et al.,[8] providing a stability analysis for an entire engine. In a slightly different approach Zhu et al.[58] used CFD to predict a flame response to several different types of input flow perturbation signals: sinusoidal, random binary, and sum of sinusoidal. Using Fourier analysis, the frequency-domain response was calculated for the input signals. Compared to a direct time-domain response at a single frequency, the different input signals provide various advantages in accuracy or computational speed to predict the transfer function. Although the results were not compared to experimental data, the predicted transfer function is a first-order response similar to Eq. (2). The analysis in Zhu et al.[58] applies to a spray flame combustor and is limited to relatively low frequencies (<120 Hz).

To use detailed models in a stability analysis, both the $\boldsymbol{G}$ and $\boldsymbol{H}$ transfer functions must be accurately known. To calculate $\boldsymbol{H}$, it is necessary to know the acoustic response of the combustor. Finite element methods have been used to predict the acoustic response,[59,60] but it is difficult to combine these acoustic analysis with predictions of the flame response, especially in combustors with multiple burners. Complications arise in situations that include coupled acoustic modes. For example, in an annular combustor both longitudinal and axial acoustic modes can be present, and the modes can be coupled. This coupling is not typically accounted for in linear acoustic models, but recent low-order models have been developed to capture this detail.[61,62] Accounting for this coupling allows an improved description of the acoustic pressures and velocities at individual burners, and it will be noted in Sec. III.B that response of individual burners should be exploited to improve stability. Pankiewitz and Sattelmayer[61] developed an acoustic model that is solved in the time domain and then specified a model for the heat release (i.e, the flame response) at the individual burner elements. Instead of using Nyquist analyis, these authors assess stability from the growth or decay of finite disturbances, similar to what has been done in rocket engine analysis.[9] An interesting result is the prediction of spinning acoustic modes in the combustion chamber, that is, the pressure nodes rotate around the annular geometry. These spinning modes have been observed in commercial annular combustors[63] and might deserve more consideration in future analysis.

In summary, Sec. II has shown how control models can be used to evaluate the stability of combustion systems. The combustion process can be treated as the forward transfer function $\boldsymbol{G}$, and the system acoustics can be represented in the feedback path $\boldsymbol{H}$. The physical processes that contribute to the combustion response were reviewed along with measurements and models that have been used to describe the transfer functions. Nyquist analysis demonstrates both the potential and problems associated with adjusting the combustion time lag to produce stability. In particular, frequency shifts and mode changes can frustrate attempts to solve a combustion dynamics problem. This will be discussed in more detail with reference to experimental data in Sec. III.

III. Time-Lag Models and Methods to Improve Combustion Stability

Various approaches have been used to improve the stability of premixed combustion systems. Examples include changes to the convective time lag,[12,13,64–66] using multiple time lags,[14,64,67] combining fuel injectors with different dynamic response,[68] changing the dynamic response of the feed system,[69,70] and adding diffusion pilot flames.[27,65] The success of these techniques can be understood from the changes to the feedback loop described in Sec. II. As already noted, simultaneous variations in flame area and fuel-air ratio can contribute to the flame dynamics. The magnitude of each contribution is usually unknown in practical problems, but it is often assumed that the fuel-air variations play a significant role, and this has been demonstrated in both experiments and engine tests.[12,13,64–66] Thus, practical solutions to dynamics problems often focus on the convective time lag τ. Relatively simple models have been successfully used to describe the effect of changes to the time lag. As will be seen, these models are a partial description of what has been shown in the Nyquist analysis. Section III.A will describe time-lag models and discuss the connection to the Nyquist analysis. Section III.B will review the effect of using multiple time lags, and Sec. III.C will describe other passive methods to improve combustion stability.

A. Time-Lag Models

In combustion dynamics the importance of various time lags is well documented in the literature, dating back to the 1950s. Putnam[41] summarized many of these ideas and used simple arguments based on Rayleigh's criterion to establish when a system will oscillate or be stable. In simple terms Rayleigh's criterion states that the heat-release perturbations q' should be in phase with pressure perturbations p' to strongly drive oscillations. Likewise, when p' and q' are out of phase oscillations are strongly damped. Consider a situation in which the fuel injector responds to sinusoidal pressure perturbations in the combustor. Assume that the local fuel-air ratio at the fuel injection location is slightly higher when combustor pressure sinusoid is at a maximum. Slightly richer perturbations are then transported downstream to the flame with a convection time lag τ. Additional time lags can characterize the combustion process (for example, the time needed to burn the reactants) and could be included in an overall time lag. For the purposes of this example, it is assumed that richer fuel perturbations arriving at the flame create an immediate increase in the heat-release rate. For the heat-release perturbation to coincide with the next pressure peak, the convective time lag τ should be equal to one acoustic period $T = 1/f$. It is also possible that the convective delay could equal two periods, three periods, etc., and the pressure and heat-release rate perturbations would still be in phase. Thus, oscillations can occur when

$$\tau/T = \tau f = 1, 2, 3, \ldots \tag{3}$$

The criterion for instability expressed by Eq. (3) is an analogue to Nyquist stability criterion described in Sec. II. Values of phase that produce encirclement of the -1 point on the real axis represent conditions in which the feedback signal arrives at the summation point and produces an amplification of the original disturbance. Equation (3) expresses the same idea: p' produces a heat-release rate variation q' that will amplify the next cycle of p' (i.e., $\tau f = 1$) or subsequent cycles ($\tau f = 2, 3, \ldots$).

The sequence $1, 2, 3 \ldots$ is specific to the simple example described. As noted by Putnam,[41] it is not necessary that the p' and q' perturbations be precisely in phase to meet the Rayleigh criterion. In principle, oscillations can occur for a range of $\tau f \pm 0.25$ centered around the indices just shown. Unlike the control model analysis, Eq. (3) does not present any information about the magnitude of the response. As such, this equation merely provides a criterion for when the phase is correct to allow oscillations to occur.

Depending on the acoustic response of both the fuel system and the air passage in the premixer, rich and lean pockets of mixture can be produced at various phase angles relative to the pressure p' in the combustor. For example, if the premixer response produces richer pockets at the minimum of the combustor pressure then only $\frac{1}{2}$ acoustic period is needed to align q' with the next maxima in pressure. Thus, the sequence would be:

$$\tau/T = \tau f = 0.5, 1.5, 2.5 \ldots \tag{4}$$

Lacking details of the premixer response, it is not known a priori what sequence of numbers will describe oscillating regions in a given application. To further complicate matters, τ is an average representation of the time from fuel injection to the time of combustion. As discussed by Lieuwen et al.,[66] this time lag depends on the flame location, as well as the flame shape. In practical systems neither are easily measured or predicted. For these reasons the sequences described in Eqs. (3) and (4) are usually considered experimentally, although some applications of computational fluid dynamics have shown promising predictions of both the time lag and the associated stability regions.[8,12,51]

Experimental evaluation of the time-lag model just described above has been demonstrated by Richards and Janus[13] and Straub and Richards.[64] A can-style combustor test rig (Fig. 10) was used to record the pressure dynamics from a premixed gas turbine fuel injector. The modular premixer design (Fig. 11) allows the position of fuel injection to be changed from three positions A, B, C, or simultaneously from two of the three positions. Thus, changes to the time lag could be studied by changing the bulk flow velocity, as well as the physical distance to the flame. Data were collected over a range of operating conditions. The time lag for each condition was estimated using a fixed flame standoff. When the observed rms pressure is plotted as a function of τf, the stability regions are clearly identified (see Fig. 12). As shown, the data indicate that oscillations are confined to a band $0.45 < \tau f < 0.7$. The edges of this region are referred to as the stability boundaries. This plot can be used to understand how proposed changes in the nozzle geometry, such as increasing the premixer length, would affect stability. For example, for a stable combustor operating at $\tau f = 0.4$, Fig. 12 indicates that proposals to move the fuel injector upstream at a fixed velocity will

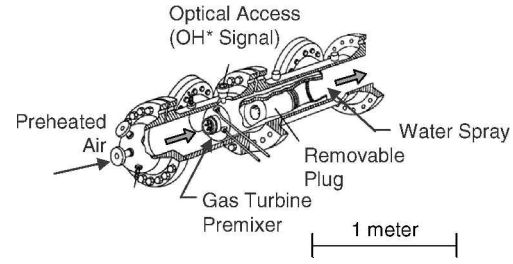

Fig. 10 Schematic of experimental combustion test rig from Ref. 13.

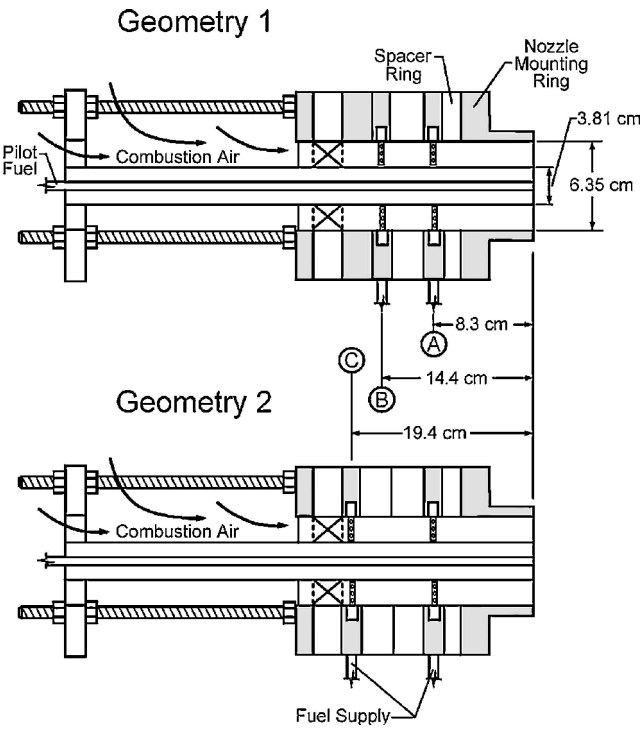

Fig. 11 Schematic of fuel-air premixer configurations used to investigate passive control approaches via changes to the time lag. Fuel-injection points A, B, and C are shown.

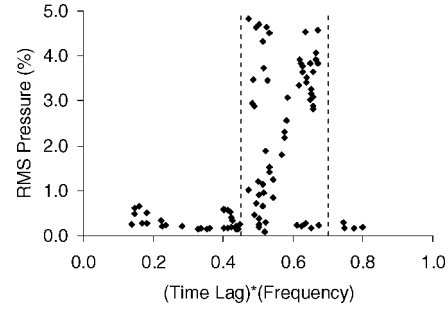

Fig. 12 Data showing the experimentally determined stability boundaries using a time-lag model from Ref. 13.

increase τf such that oscillations will occur. This has been demonstrated experimentally by Richards and Janus.[13] It would also be possible (but not necessarily advisable) to increase the fuel time lag enough to get to the upper stability boundary. This has been shown experimentally by Straub and Richards[64] and will be discussed in more detail later.

It is useful to understand how the τf plot and the control model analysis in Sec. II are related. In Sec. II, the Nyquist analysis shows how changing time lags rotate the lobes of the plot to include encirclement of -1. These encirclements represent conditions where the heat-release rate and pressure perturbations have the correct phase and adequate gain to produce instability. Increasing τ rotates the lobe until encirclement occurs at a particular frequency (say, f_1), and further increases in the time lag continue the rotation of the Nyquist plot until the lobe does not encircle -1 at a lower frequency (say, f_2). The stability boundary in the τf plot also represents the conditions where p' and q' have the correct gain/phase to produce instability. It is sometimes overlooked, or misunderstood, that the right and left stability boundaries in the τf plot must therefore have decreasing frequencies ($f_2 < f_1$). Attempts to solve instability problems by adjusting the time lag must recognize that the frequency will change in response to changes in the time lag. The Nyquist analysis indicates this very clearly. If the bandwidth of the acoustic response is very large, the lobe of the Nyquist plot covers a wide frequency range, and significant changes in the value of τ are needed to cross the stability boundaries. Fannin et al.[29] showed a more detailed comparison between the Nyquist stability boundaries and the simple time-lag model.

Multiple acoustic modes introduce another complication to the time-lag model. When the system acoustics produce strong response at several frequencies, changes to the time lag can jump between frequencies, rather than produce stability. This point has been demonstrated in the example Nyquist plots shown in Sec. II, where subsequent lobes of the Nyquist diagram rotate and encircle -1 as the time lag is increased (or decreased). The concept can also be described less formally by a plot like Fig. 13. In Fig. 13 frequency is plotted on the vertical axis, and the time lag is plotted on the horizontal axis. The indices where instability occurs are plotted as regions having a 0.25 width, that is, $0.5 < \tau f < 0.75$, etc. Horizontal lines are drawn through combustor natural acoustic frequencies as shown. Combinations of τf within the instability regions have the correct phase to meet the Rayleigh criterion and can therefore oscillate. If a given combustor exhibits oscillations at frequency f_1 with $\tau = 1$ ms, a proposed solution might be to increase the time lag. However, as shown, this solution has the potential to get to the edge of the stability boundary $\tau f_1 = 0.75$ and then drop to $\tau f_2 = 0.50$. It is conceivable that continued increases in time lag to $\sim$2 ms could produce stability, but slightly greater time lag could then jump back to $\tau f_1 = 1.50$ or $\tau f_3 = 0.50$ Thus, adjustment of the time lag must be carried out with a full understanding of the frequency spacing of acoustic modes. Figure 13 suggests that closely spaced natural

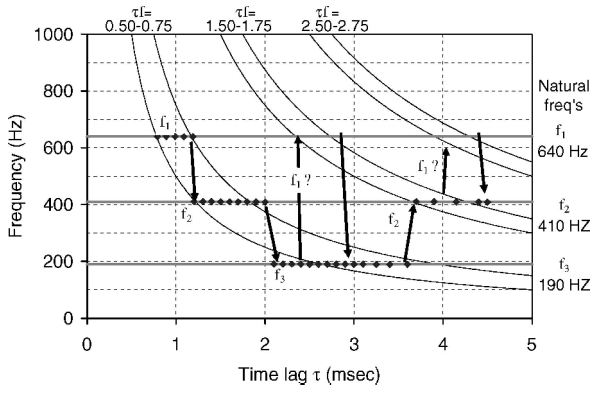

Fig. 13 Stability boundaries of the time-lag model plotted as frequency vs time lag. Also shown are three different frequency modes that can complicate approaches to control combustion oscillations by changing the time lag.

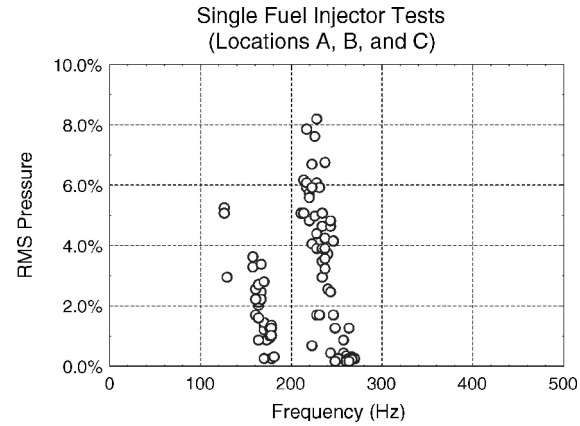

Fig. 14 Experimental data showing multiple frequency modes.

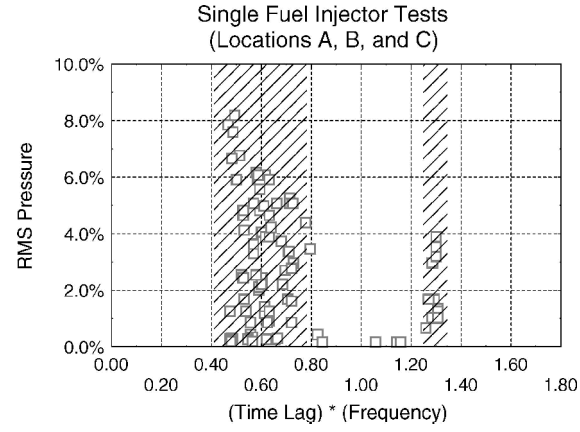

Fig. 15 Data showing experimentally determined stability boundaries for multiple-frequency-mode combustor using the time-lag model.

frequencies can lead to many transitions between oscillating conditions over a wide range of time lag values. A similar conclusion can be drawn from the formal Nyquist analysis, where multiple natural frequencies produce multiple lobes on the Nyquist diagram.

Experimental demonstration of the frequency switching behavior just described has been presented by Straub and Richards.[64] The modular fuel injector (Fig. 11) was studied over a range of bulk velocities (30–60 m/s) and with different fuel-injection positions A, B, or C. This produced a net variation in time lag from 1.8 to 7.3 ms. Figure 14 is a plot of all of the experimental data and shows that this combustor has two strongly responsive frequencies near 160 and 220 Hz. Based on calculations, these frequencies are close to (but not equal to) the natural frequencies expected for the combustor. (As discussed in Sec. II.A, the observed limit-cycle frequencies will differ from the acoustic natural frequencies.) The rms pressure data are shown in Fig. 15 plotted against the τf product. As expected, oscillations were confined to relatively small regions of the τf plot, in spite of the multiple acoustic modes and the wide range of time lags investigated. There are few data points in the stable region between the τf peaks. This is an example of the frequency switching shown schematically in Fig. 13. To clarify this point, Fig. 16 shows the dominant frequency of oscillation plotted as a function of the time lag for nozzle configuration C and a range of equivalence ratio conditions. As the time lag increases, the frequency drops slightly, and the stability boundary for $\tau f = 0.80$ is approached. At this condition the rms pressure levels were strongly dependent on the equivalence ratio; weak oscillations near 260 Hz were exchanged with strong oscillations at 160 Hz as the equivalence ratio was changed. Further increases in time lag caused an increase in frequency and moved the system to the next τf band, where the amplitude was again large. Still further increases in time lag were accompanied by a reduction in oscillating frequency. All of the experimental observations are consistent with both the time-lag model and the Nyquist analysis

presented in Sec. II. However, contrary to the time-lag model that only considers the timing (phase) of the system, the Nyquist analysis incorporates both the gain and the phase of the system.

The preceding discussion has shown that solving dynamics problems by adjusting the time lag can be complicated by the multiple τf bands and multiple acoustic modes. If the frequency spacing Δf between adjacent acoustic modes is such that mode transitions are possible (as in Fig. 13), there is a good chance that changing the time lag will simply produce a frequency shift, rather than stable combustion. This conclusion depends on the gain of the various modes, but it does suggests the following rule of thumb: where the mode spacing Δf is such that $\Delta f \tau \sim <0.5$, changes in the time lag can lead to mode switching. In these instances rather than modifying τ to produce stability, consideration should be given to increasing the time-lag distribution (Sec. III.B) or modifying the acoustic response of the combustor (Sec. IV).

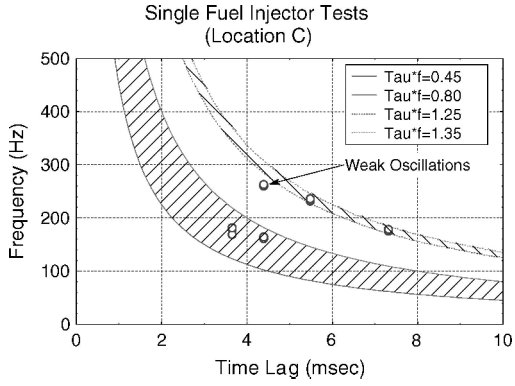

Fig. 16 Experimental data showing transition between τf bands and different frequencies.

B. Improving Stability by Increasing the Time-Lag Distribution

The preceding discussion shows how discrete times lags affect system stability. A related issue is the influence of multiple time lags. The concept was noted by Keller[14] and is the subject of a commercial patent.[71] Multiple time lags could be produced using two (or more) points of axial fuel injection simultaneously (i.e., positions A and B or A and C, shown in Fig. 11). Both fuel-injection points produce rich and lean pockets of premix fuel in response to premix airflow. Only one of the pockets can produce heat-release rate perturbations that are in phase with the pressure; the other pocket can be arranged to produce perturbations that are out of phase with the acoustic pressure, adding damping. The benefit of this approach has been demonstrated experimentally in Straub and Richards,[64] where single-point injection is compared to multiple-point injection using the geometry shown in Fig. 11. The resulting stability maps are shown in Fig. 17. The horizontal axes are the equivalence ratio and bulk premixer velocity. The vertical height represents the

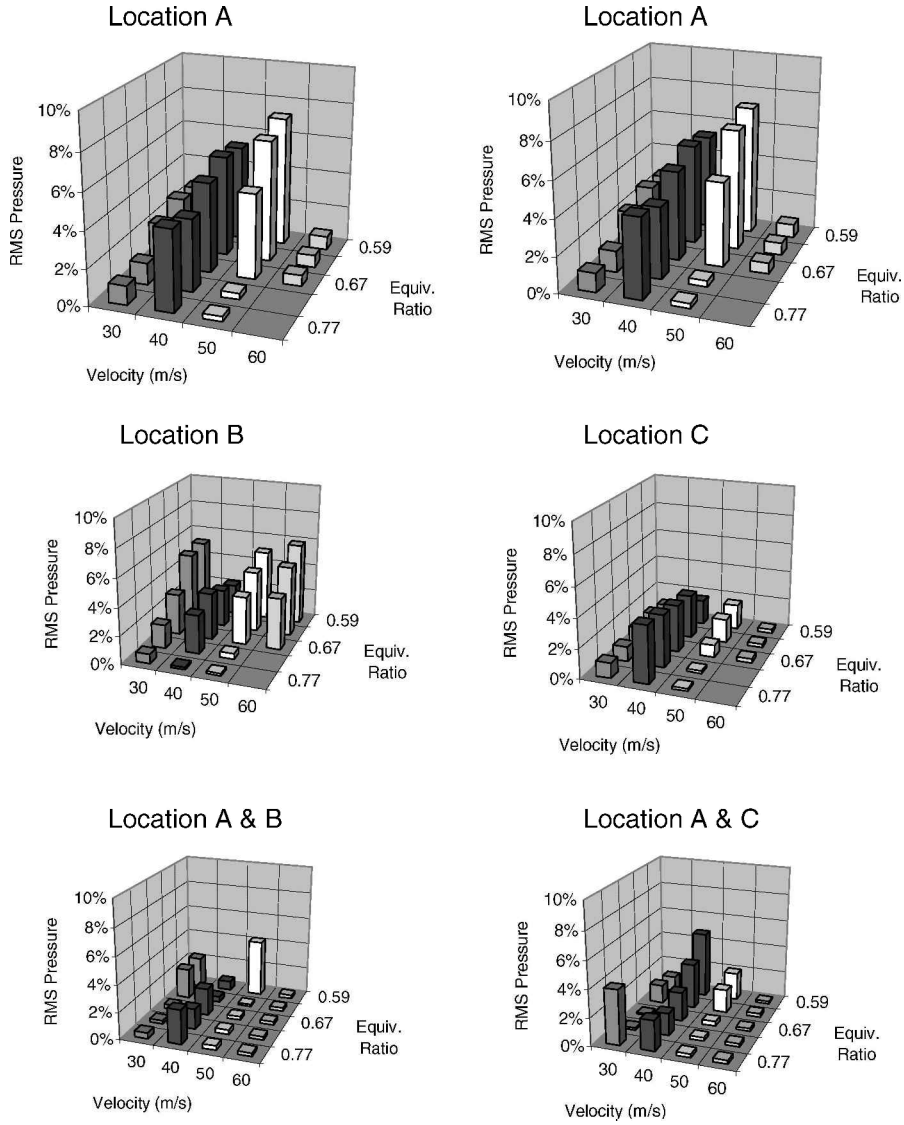

Fig. 17 Experimental data showing the effect of changing the distribution of time lag by using fuel injection from two axial locations, A and B and A and C in Fig. 11.

rms level of the pressure oscillation. Note that injection from points A, B, or C had almost universally higher amplitudes than simultaneous injection from points A and B or A and C. Fannin et al.[29] investigated these experimental results using Nyquist analysis to demonstrate that the multiple time lags can produce a significant reduction in oscillating pressure, as seen in the data. The Nyquist analysis shows that multiple time delays produce a reduction in the amplitude of the mixture ratio perturbations, as well as adjustment to the phase.

An interesting practical application of the multiple time-lag concept was carried out by Berenbrink and Hoffmann.[68] These authors recognized that the time lags can be adjusted on individual fuel injectors so that the combined combustion response benefits from different time lags associated with the individual injectors. This has an advantage compared to placing multiple fuel ports in a single injector (Fig. 11) because it is easier to optimize the mixing from a single fuel port. On a combustor with 24 fuel injectors, a total of 20 injectors were outfitted with extension tubes that produced different time lags. The resulting engine test demonstrated that it was possible to operate the engine at conditions that had previously been limited by dynamic oscillations. In addition, a slightly different approach using asymmetric burners was also shown to produce comparable stabilization. The asymmetric burner concept simply placed different fuel injectors at different angles relative to the combustor flow axis. The resulting asymmetry in the flame shape prevents uniform coupling to the acoustic and also has the effect of shifting the flame position on different oriented injectors. The net effect is again a distribution of time lags among the different injectors.

Lovett and Uznanski[67] used a different concept to produce multiple time lags in a single fuel injector. Their approach allowed a split between fuel supplied to a main and secondary premixer passage, with each passage having a unique time lag. In this manner a composite response could be achieved by adjusting the flow splits. This approach produced reduced dynamics at select values of the secondary fuel flow.

Deliberate introduction of multiple time lags is one method to reduce the contribution of fuel-air perturbations to oscillating heat-release rate. A second approach is to simply take advantage of the mixing processes that occur during fuel injection. Because the fuel-air perturbations are mixed by turbulent processes in the premixer, a single time lag does not completely describe the premixer response to flow perturbation. To account for turbulent mixing, a distribution of time lags will better represent the response of even a single point of fuel injection. Scarinci and Freeman[45] showed that turbulence in the premixer can significantly disperse fuel-air perturbations and suggest that dispersion can reduce the oscillating amplitude of combustors using longer premixer barrels. Sattelmayer[46] has shown that the time-lag distribution can play a key role in reducing the overall magnitude of the heat-release oscillation. Thus, attempts to improve stability should recognize the contribution of time-lag distribution in the premixing process and also from the geometry of the flame, discussed next.

C. Flame Dynamics and Flame Geometry

Although the time-lag distribution is beneficial at reducing the impact of the fuel-air perturbations, it must also be recognized that this feature is only a guaranteed benefit when perturbations are the sole cause of instability. This might not be the case in many instances because even fully premixed flames can exhibit dynamic response to variations in mixture flow. As discussed in Sec. II.B, unsteady aerodynamics can produce a variation in heat release as a result of changes in flame area or vortex shedding/merging. These flame dynamics can occur without any perturbations in fuel-air ratio. In these instances a Nyquist analysis would show that adding fuel-air perturbations could silence the oscillation that is produced by the flame area variation. This is the basis for active combustion control using input fuel perturbations. The active control system changes the magnitude and phase of the fuel system feedback, producing stability by controlling the arrival of mechanically actuated fuel perturbations. A similar idea has been demonstrated by making passive adjustments to the feed system dynamics, producing stability at select conditions by controlling the arrival of fuel-air perturbations.[43,69,70]

Another consideration in describing the flame response is the geometry of the flame. Even if the flame is treated as having a static configuration, the arrival of fuel-air perturbations is distributed over the surface of what is typically a conical flame geometry. The conic geometry means that the delivery of a fuel perturbation will produce a combustion response that is distributed over the surface of the flame. Putnam[41] recognized that these geometric features could be accounted with a correction to a time lag by integrating over the surface of the flame. More recently, Lieuwen et al.[66] developed a similar integral analysis and applied it directly to flame geometries that are of interest to gas turbine combustors. This analysis showed that correction factors to the time lag can be as large as a factor of 1.5, and the correction is shown to be fairly sensitive to the shape of the flame. Because of the uncertainties connected with describing the position and shape of turbine combustion flames, rig measurements of the time lag are probably needed to describe the details of practical flame response. Straub et al.[72] have made preliminary attempts to measure the flame time lag in a practical scale combustor, but more work is needed on this topic. Krebs et al.[51] measured the time lag in an atmospheric pressure model of a gas turbine combustor and showed that a time-lag distribution was needed to describe the measured response. The distribution is needed to account for the geometry of the flame.

Flame anchoring is another consideration for reducing the flame dynamics. As mentioned in Sec. II.B, Kendrick et al.[26] suggest that poor flame anchoring can allow combustion to oscillate or anchor in a location where the time lag will favorably drive oscillations. Paschereit et al.[27] showed that an oscillating flame anchor was responsible for driving dynamics in their combustion system. This problem was solved by physically locating a pilot flame in the region where positive flame anchoring was needed. The addition of a pilot flame is a common approach to reducing flame dynamics,[26] but the stabilizing mechanism is often uncertain. Both Kendrick et al.[26] and Paschereit et al.[27] attribute pilot-enhanced stability to an improvement in flame anchoring, but there are additional reasons why pilots can improve stability. The pilot flame is typically operated as a diffusion flame, or partially premixed, and it can have a lower dynamic response than a purely premixed flame. In a diffusion flame, the local reaction rate is controlled by mixing, not the overall fuel-air ratio. Thus, momentary perturbations in the fuel or air supply cannot produce an appreciable change in the reaction rate. This reduces the likelihood of oscillations in diffusion flames and might explain why diffusion pilots can be used to silence oscillations. Although more work is needed to understand the stabilizing effect of pilot flames, diffusion pilot flames are very undesirable because they contribute significantly to NOx emissions.

IV. Acoustic Dampers

In the turbine combustion literature passive control methods are strongly weighted toward stabilizing the combustion process. Less emphasis has been given to the use of acoustic dampers. This is surprising because acoustic dampers are commonly used to stabilize rocket and afterburner applications and have proven very effective when properly designed. In stationary engines the disparity of damper use can be related to the relatively low frequencies encountered in turbine applications (hundreds of hertz) vs those typically damped in rocket engines (kilohertz range). The lower frequencies require physically larger dampers, complicating engine packaging, and this is a potential drawback. Nevertheless, dampers should not be overlooked in a strategy to stabilize combustion. Given the difficulty of proposing changes to the combustion response (the $\boldsymbol{G}$ transfer function; Fig. 1), a damper design can be proposed that will very likely reduce acoustic feedback (the $\boldsymbol{H}$ transfer function; Fig. 1). This is not to imply that damper design is easy or without uncertainties. However, given the cost of reengineering a combustion system to produce a desired combustion response, addition of dampers might be a worthwhile consideration. These dampers are described next.

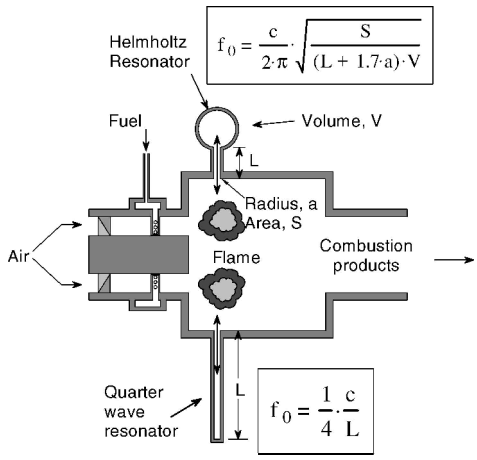

Fig. 18 Schematic of resonator concepts to dampen the acoustic feedback of the combustion system.

A. Damper Description

The simplest damper of all is a hole, releasing acoustic energy from the combustion chamber that would otherwise return to the feedback loop. The efficacy of this method is well known to practicing combustion engineers. Putnam[41] noted the following advice for practitioners faced with stubborn oscillation problems in industrial burners: "To solve an oscillating combustion problem, drill a hole. If that doesn't work, drill two holes."

Although this is a humorous anecdote, it represents genuine experience that reducing the acoustic gain can stabilize oscillating systems. Conversely, eliminating holes can lead to instability. Modern premixed combustors are designed specifically to avoid dilution holes, removing a source of acoustic damping. This is yet another reason why premixed combustors tend to have problems with dynamics. Earlier diffusion flame combustors used numerous dilution holes around the perimeter of the liner, providing a source of acoustic damping that is absent in premixed combustors.

Although drilling holes might be an acceptable control strategy in industrial burners, it is not an option for gas turbine combustors where flow splits must be accurately controlled to meet performance targets. Instead, closed resonators can be used to absorb acoustic energy. Because the resonators are closed, they do not compromise the designed flow splits. These type of resonators have been used extensively in rockets[9,73] and afterburners.[74] Figure 18 shows two common resonator geometries that have been used in gas turbine applications: the Helmholtz and quarter-wave resonator; the latter often referred to as a quarter-wave tube. Both types are shown for convenience on a single combustor, but are not necessarily combined in practice. Figure 18 also shows the formulas and nomenclature used to calculate the natural frequency f_0 of the resonator.

When pressure oscillations occur, flow enters and exits the resonator mouth. Acoustic energy is dissipated in the entrance/exit losses, providing damping to the system. It can be shown[9] that the greatest losses are generated by maximizing the magnitude of the oscillating velocity; this is achieved by tuning the resonator so that the natural frequency f_0 is close to the frequency that is to be damped in the combustor. For a given f_0, the Helmholtz neck area S can be traded with the length L and volume V to meet packaging space requirements. In the quarter-wave design f_0 can only be established by the length.

The actual performance of a resonator depends on the resonator geometry and the operating conditions. Because the acoustic dissipation occurs at the entrance/exit flow near the mouth, the geometry of this region is very important. Laudien et al.[73] show that rounded vs square corners at the resonator/combustor connection produce a significant difference in the acoustic response. Furthermore, because the resonator gas can include combustor products and purge cooling gas the speed of sound is uncertain, making it difficult to design the resonator for a specific natural frequency. Thus, resonator design and tuning is not usually achieved from analysis alone. In most rocket applications, as well as the few turbine applications cited next, the resonator properties are finalized by experimental testing.

Selecting the position and number of resonators is also an important consideration. It does little good to place the resonator at an acoustic node. For example, in annular combustors circumferential acoustic modes (with waves traveling around the annulus) are often characterized by standing nodes at specific positions. Resonators added at these node positions will not provide damping; there is no acoustic pressure to drive the oscillator. Attempts to position resonators at the pressure antinodes might be frustrated by a repositioning of the node to the new resonator location. Thus, it can be essential to position multiple resonators using the number of resonators that are guaranteed to produce an asymmetry relative to the acoustic mode shape. For example, three resonators cannot all be aligned with a wave structure having only two nodes. Decisions about the number of resonators are made based on an analysis of acoustic waveform and the required damping in specific situations. Some examples are described in Sec. IV.B.

B. Application of Acoustic Dampers on Stationary Gas Turbines

Gysling et al.[75] examined the use of Helmholtz resonators on a sector rig combustor. Their analysis identified many of the important design variables for installing a resonator: the ratio of the resonator to combustor volume, the resonator frequency, and the loss coefficient at the resonator mouth. The final resonator performance was characterized by measuring the performance in situ. This was accomplished by measuring the transfer function between the combustion chamber pressure and the resonator pressure and then fitting the theoretical parameters to the resulting data. The authors point out that this fit was made at each operating condition of interest. As just noted, the gas temperature and flow conditions in the combustor will affect the resonator natural frequency and damping; this needs to be accounted for in resonator performance.

Five resonator configurations and three test conditions were reported by Gysling et al.[75] In the best cases, appropriately tuned resonators reduced the oscillating pressure by almost an order of magnitude. The required resonator volume was 12% of the combustion chamber volume. Based on both theoretical modeling and experimental data, these authors also identify many of the important considerations for resonator use. Because a given engine can experience a frequency shift with operating conditions, the resonator system must provide damping over a range of frequencies. This can be accomplished by mistuning the resonator or using multiple resonators tuned to different frequencies. This approach provides less than maximum damping at a single frequency, but allows good performance over the range of conditions. In Gysling et al.[75] this was successfully demonstrated using two resonators tuned to two different frequencies. Good attenuation was observed on this combustor application where oscillating frequencies ranged from 232 to 278 Hz.

Bellucci et al.[76] used a Helmholtz resonator model to design dampers that were added to the silo combustor of a stationary gas turbine. The resonator model included more physical detail for loss mechanisms than in Gysling et al.[75] Experimental testing was again used to establish the model parameters and then design resonators for the actual combustion system. A total of seven resonators were installed at the inlet end of the combustor. The pressure oscillation amplitude was reduced by about 60% compared to the baseline without resonators. This paper did not report the resonator performance at other frequencies or operating conditions. The authors also used a supply of purge gas to keep the resonator temperature low.

As a final example of the use of resonators, Pandalai and Mongia[3] report on the use of acoustic dampers on aeroderivative engine applications. Unlike the prior citations, these authors installed the damper tubes upstream of the combustor, just prior to the fuel-air mixer. The damper tubes were constructed from 25.4-mm tubes. A perforated plate at the resonator mouth was used to control the resonator impedance. Although these authors do not compare

the oscillating pressure with or without the damper tubes, it is noted that these dampers are now in wide commercial use, having logged more than 100,000 h of operation in various engine installation. This is an excellent example of how dampers can play a significant role in reducing pressure oscillations in stationary engines.

A few words of clarification are made before concluding this discussion of acoustic dampers. It is sometimes overlooked that dampers themselves participate in the overall acoustic response of the combustion chamber. When dampers with sufficient mouth area represent a considerable portion of the combustor volume, their presence can lead to a change in the natural frequency of the entire combustion system, and they can actually destabilize an otherwise stable system. This possibility was noted by Gysling et al.[75] and should be carefully considered before sizing and tuning resonators. Mitchell[77] notes that in rocket damper applications sizing the resonators apart from understanding the acoustic structure in the combustor can lead to less than optimal results. Mitchell provides an example where the greatest stability was achieved with mistuning the resonator from the oscillating frequency; this was attributed to the change in waveform that accompanied addition of the resonators.

V. Summary

This paper reviews the status of passive control methods for stabilizing premixed combustion in gas turbines. Feedback control models reviewed in Sec. II show how both the flame transfer function and the feedback acoustics are linked together in a dynamics problem. Nyquist analysis illustrates how multiple acoustic modes can confound approaches to eliminate combustion instabilities by changing the time lag. The physical processes affecting the flame response are reviewed, and some examples of the complex details of practical flame transfer functions are provided. In Sec. III, applications of time-lag modifications are presented, and the limitations of this approach are also discussed. Experimental results demonstrating frequency shifts predicted by the Nyquist analysis are shown. The stabilizing effect of time-lag distribution is discussed, along with some field applications that confirm the beneficial effect of using time-lag distributions. Improvements to stability from flame anchoring modifications and pilot flames are also reviewed. In Sec. IV, a review of acoustic damping suggests that dampers can be used effectively to stabilize premixed combustion. A small number of lab-scale and fielded-engine studies are reviewed, showing excellent attenuation from the dampers.

In closing, it is interesting to speculate on the potential situations where dynamics might be a concern in future gas turbine engine applications. It is often assumed that dynamics problems are limited to stationary gas turbines, using premixed combustion. However, recent experiences with two different integrated gasification combined-cycle power plants suffered dynamics problems well into engine commissioning.[78] The trend for most advanced power generators and aeroengine applications is to raise the operating pressure to enhance efficiency. At the same time it is desirable to reduce the cooling and dilution flows to enhance performance or reduce emissions. The higher operating pressures release more heat in the same volume, increasing the magnitude of heat-release rate perturbations. The reduction in dilution or cooling flows also reduces the acoustic losses from the combustion liner. These combined features raise the potential for dynamics. Thus, it seems likely that the prominence of this problem will continue to be an issue. A combination of passive control strategies outlined here, as well as emerging active control strategies (described elsewhere in this issue), offers an opportunity to mitigate these problems as new systems are designed.

Appendix: Derivation of Transfer Functions

This Appendix documents the calculations used in the generation of Figs. 5–8. The acoustic computations are described first, followed by a derivation of the response of the system to a velocity source located at the flame, and incorporation of a flame model to yield the ***H*** transfer function.

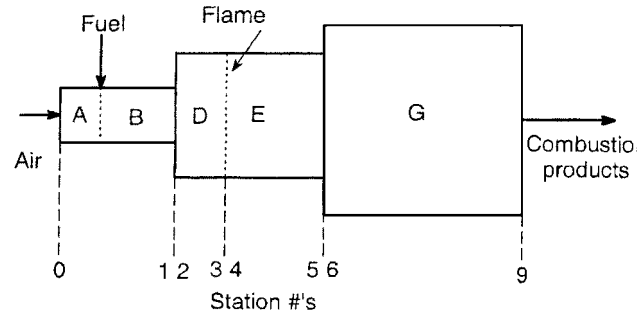

Fig. A1 Generic combustor geometry (not to scale).

A "generic" combustor geometry is shown in Fig. A1. The premix injector is depicted by regions A and B, with air entering at the upstream side of region A and fuel entering in the plane between regions A and B. The computations described here do not include the dynamics of air and fuel mixing explicitly, and so the injector region will be referred to jointly as AB. The air/fuel mixture enters the combustion chamber at region D, where it continues to flow downstream a short distance before burning in the plane between regions D and E. In the two-mode system described in the paper, a step expansion was placed at the interface between regions E and G. Computation stations, numbered 0–9, are also shown in Fig. A1. To simplify the calculations, "hard" acoustic boundaries were assumed to exist at stations 0 and 9 (i.e., the acoustic velocity is zero). The specific geometry and other conditions used in the calculations for the two-mode system are listed in the Table A1.

The acoustic properties of the combustor model are described by the acoustic impedances. Impedance is the complex ratio of acoustic pressure to mass velocity at each station. The impedance at each station was computed through use of acoustic transfer matrices. These matrices of complex numbers relate the acoustic pressure and velocity at one station to that at the next and are a function of the geometry and the local gas conditions. For example,

$$\begin{pmatrix} p_1 \\ v_1 \end{pmatrix} = C \cdot \begin{pmatrix} p_2 \\ v_2 \end{pmatrix}, \qquad \begin{pmatrix} p_0 \\ v_0 \end{pmatrix} = AB \cdot \begin{pmatrix} p_1 \\ v_1 \end{pmatrix}$$

$$\text{and} \quad \begin{pmatrix} p_2 \\ v_2 \end{pmatrix} = D \cdot \begin{pmatrix} p_3 \\ v_3 \end{pmatrix} \qquad \text{(A1, A2, and A3)}$$

The acoustic pressures p and velocities v are represented by complex phasors, with both amplitude and phase. The 2×2 matrices AB, C, and D are acoustic transfer matrices for their respective regions. The matrices C and F do not correspond to specific regions but represent the acoustic transfer matrices for the step expansions that occur between regions AB and D and regions E and G, respectively. The acoustic pressure and velocity at a particular station are a linear function of those at the next station downstream. A similar linear relationship does not exist between stations 3 and 4 because of the presence of the flame, which acts as an acoustic source.

The 2×2 acoustic transfer matrices for various geometries are defined in Munjal.[28] For simple cylindrical elements

$$R(s, L, \mu, f, c) = \begin{pmatrix} \cos\left(\dfrac{2 \cdot \pi \cdot f \cdot L}{c}\right) & \dfrac{j \cdot c}{s} \sin\left(\dfrac{2 \cdot \pi \cdot f \cdot L}{c}\right) \\ \dfrac{j \cdot s}{c} \sin\left(\dfrac{2 \cdot \pi \cdot f \cdot L}{c}\right) & \cos\left(\dfrac{2 \cdot \pi \cdot f \cdot L}{c}\right) \end{pmatrix} \cdot e^{(-j(\mu/c)(2 \cdot \pi \cdot f/c))} \qquad \text{(A4)}$$

Table A1 Geometry and gas conditions used in the two-mode combustor model

Geometric region	Dual-mode combustor simulation parameters			
	A+B	D	E	G
Diameter, m	0.06858	0.13335	0.13335	0.17780
Length, m	0.06350	0.01270	1.39700	0.63500
Area, m^2	0.003694	0.013966	0.013966	0.024829
Temperature, K	533.3	533.3	1811.1	1811.3
Pressure, Pa	2,020,000	2,020,000	2,020,000	2,020,895
Density, kg/m^3	13.21	13.21	3.89	3.89
Gamma	1.4	1.4	1.3	1.3
Mol. wt., kg/kg-mole	29	29	29	29
c, m/s	462.7	462.7	821.6	821.6
U, m/s	28.87	7.64	25.93	14.58
Mach no.	0.06240	0.01651	0.03156	0.01775
Mass flow, kg/s	1.409	1.409	1.409	1.409
Boundary conditions				
p_{in}	——	——	$p_4 = p_3$	——
v_{in}	$v_0 = 0$	——	——	——
p_{out}	——	$p_3 = p_4$	$v_4 = v_3 \cdot \frac{\rho_4}{\rho_3} + v_s$	——
v_{out}	——	——	——	$v_9 = 0$

For step expansions such as that between stations 1 and 2, the transfer matrix is

$$S(\zeta_a, \zeta_b, M_a, M_b, k, \gamma) := \begin{pmatrix} 1 & M_b \cdot \zeta_b \\ \frac{M_b}{\zeta_b} & 1 \end{pmatrix}^{-1} \cdot \begin{bmatrix} 1 - \frac{k \cdot M_a^2}{1 - M_a^2} & \frac{k \cdot M_a \cdot \zeta_a}{1 - M_a^2} \\ \frac{(\gamma - 1) \cdot k \cdot M_a^3}{\left(1 - M_a^2\right) \cdot \zeta_a} & 1 - \frac{(\gamma - 1) \cdot k \cdot M_a^2}{1 - M_a^2} \end{bmatrix} \cdot \begin{pmatrix} 1 & M_a \cdot \zeta_a \\ \frac{M_a}{\zeta_a} & 1 \end{pmatrix} \tag{A5}$$

where k is

$$k = \left(\frac{s_b}{s_a} - 1\right)^2 \tag{A6}$$

The acoustic impedances at each station in the model were calculated starting from known boundary conditions. At station 0, $v_0 = 0$ such that

$$Z_0 = p_0 / v_0 = \infty \tag{A7}$$

At station 1, $v_0 = 0 = AB_{1,0} * p_1 + AB_{1,1} * v_1$, which implies

$$Z_1 = p_1 / v_1 = -AB_{1,1} / AB_{1,0} \tag{A8}$$

At station 2,

$$Z_1 = \frac{p_1}{v_1} = \frac{C_{0,0} \cdot p_2 + C_{0,1} \cdot v_2}{C_{1,0} \cdot p_2 + C_{1,1} \cdot v_2} \cdot \frac{(1/v_2)}{(1/v_2)} = \frac{C_{0,0} \cdot Z_2 + C_{0,1}}{C_{1,0} \cdot Z_2 + C_{1,1}}$$

therefore

$$Z_2 = \frac{-(Z_1 \cdot C_{1,1} - C_{0,1})}{(Z_1 \cdot C_{1,0} - C_{0,0})} \tag{A9}$$

And, similarly at station 3

$$Z_3 = \frac{-(Z_2 \cdot D_{1,1} - D_{0,1})}{(Z_2 \cdot D_{1,0} - D_{0,0})} \tag{A10}$$

At station 9, $v_9 = 0$ such that

$$Z_9 = p_9 / v_9 = \infty \tag{A11}$$

At station 6

$$Z_6 = \frac{p_6}{v_6} = \frac{G_{0,0} \cdot p_9 + G_{0,1} \cdot v_9}{G_{1,0} \cdot p_9 + G_{1,1} \cdot v_9} = \frac{G_{0,0}}{G_{1,0}} \tag{A12}$$

At station 5

$$Z_5 = \frac{p_5}{v_5} = \frac{F_{0,0} \cdot p_6 + F_{0,1} \cdot v_6}{F_{1,0} \cdot p_6 + F_{1,1} \cdot v_6} = \frac{F_{0,0} \cdot Z_6 + F_{0,1}}{F_{1,0} \cdot Z_6 + F_{1,1}} \tag{A13}$$

And at station 4

$$Z_4 = \frac{E_{0,0} \cdot Z_5 + E_{0,1}}{E_{1,0} \cdot Z_5 + E_{1,1}} \tag{A14}$$

The flame was modeled as an acoustic velocity source located in the plane between stations 3 and 4. The boundary conditions at this interface are $p_3 = p_4$ and $v_4 = v_3 * (\rho_4/\rho_3) + v_s$. The transfer function relating the acoustic pressure to the velocity source, that is,

$$\psi = \frac{p_3}{v_s} \tag{A15}$$

was derived in terms of system impedances, starting with the definition of the impedance at station 4:

$$Z_4 = \frac{p_4}{v_4} = \frac{p_3}{v_3 \cdot (\rho_4/\rho_3) + v_s} = \frac{p_3}{v_3 \cdot (\rho_4/\rho_3) + v_s} \cdot \frac{(1/p_3)}{(1/p_3)} = \frac{1}{(1/Z_3) \cdot (\rho_4/\rho_3) + (1/\psi)} \tag{A16}$$

Therefore,

$$\psi = \frac{Z_3 \cdot Z_4}{Z_3 - (\rho_4/\rho_3) \cdot Z_4} \tag{A17}$$

The transfer function relating acoustic pressure to variations in heat release was derived by relating heat release and an acoustic velocity source (see Schuermans et al.[25]).

$$v_s = \frac{p_3}{\psi} = \left[\rho_4 \cdot \left(\frac{T_4}{T_3} - 1\right) \cdot \mu_3 \cdot s_3\right] \cdot \frac{q'}{Q} + \left[\rho_4 \cdot \left(\frac{T_4}{T_3} - 1\right) \cdot \mu_3 \cdot s_3\right] \cdot \frac{p_3}{P_3} \tag{A18}$$

Equation (A18) provides the last link needed to derive $\boldsymbol{H}$, the relative pressure response to oscillations in heat release. Derivation of the $\boldsymbol{H}$ transfer function started with Eq. (A18) by separating terms involving p_3 from v_3 and dividing through by P_3 to yield

$$\frac{p_3}{P_3}\cdot\left\{\frac{1}{\psi}-\frac{1}{P_3}\cdot\left[\rho_4\cdot\left(\frac{T_4}{T_3}-1\right)\cdot\mu_3\cdot s_3\right]\right\} = \frac{q'}{Q}\cdot\left[\rho_4\cdot\left(\frac{T_4}{T_3}-1\right)\cdot\frac{\mu_3\cdot s_3}{P_3}\right] \tag{A19}$$

Therefore,

$$\boldsymbol{H}=\frac{p_3}{P_3}\Big/\frac{q'}{Q}=\left[\rho_4\cdot\left(\frac{T_4}{T_3}-1\right)\cdot\frac{\mu_3\cdot s_3}{P_3}\right]\Big/\left[\frac{1}{\psi}-\frac{1}{P_3}\cdot\left[\rho_4\cdot\left[\rho_4\cdot\left(\frac{T_4}{T_3}-1\right)\cdot\mu_3\cdot s_3\right]\right]\right] \tag{A20}$$

A simple form for transfer function $\boldsymbol{G}$, the relative heat release response to pressure fluctuations, was assumed in order to compute the open-loop response function. The function $\boldsymbol{G}$ was assumed to be a simple time lag. The time-lag model is shown next with a gain of $\frac{1}{2}$:

$$\boldsymbol{G}=\frac{q'}{Q}\Big/\frac{p_3}{P_3}=\frac{1}{2}\cdot e^{-1j\cdot\omega\cdot\tau} \tag{A21}$$

The gain and time lag of function $\boldsymbol{G}$ can be varied according to the situation being modeled. These equations for $\boldsymbol{G}$ and $\boldsymbol{H}$ were used to compute the open-loop response functions $\boldsymbol{G}*\boldsymbol{H}$ for the example Bode and Nyquist plots discussed in the body of the paper.

Acknowledgments

The authors wish to acknowledge many helpful discussions with colleagues at Virginia Polytechnic Institute and State University, Blacksburg, Virginia (Will Saunders, Bill Baumann, and Uri Vandsburger) who encouraged the use of feedback control modeling. Funding support from the U.S. Department of Energy National Energy Technology Laboratory is gratefully recognized.

References

[1]Hobson, D. E., Fackrell, J. E., and Hewitt, G., "Combustion Instabilities in Industrial Gas Turbines—Measurements on Operating Plant and Thermoacoustic Modeling," *Journal of Engineering for Gas Turbines and Power*, Vol. 122, No. 3, 2000, pp. 420–428.

[2]Sholz, M. H., and Depietro, S. M., "Field Experience on DLN Typhoon Industrial Gas Turbines," American Society of Mechanical Engineers, Paper 97-GT-61, June 1997.

[3]Pandalai, R. P., and Mongia, H. C., "Combustion Instability Characteristics of Industrial Engine Dry Low Emission Combustion Systems," AIAA Paper 98-3379, July 1998.

[4]Seume, J. R., Vortmeyer, N., Krause, W., Hermann, J., Hantschk, C.-C., Zangl, P., Gleis, S., Vortmeyer, D., and Orthmann, A., "Application of Active Combustion Instability Control to a Heavy Duty Gas Turbine," *Journal of Engineering for Gas Turbines and Power*, Vol. 120, No. 4, 1998, pp. 721–726.

[5]Chu, B. T., "On the Generation of Pressure Waves at a Plane Flame Front," *Proceedings of the Combustion Institute*, Vol. 4., 1953, pp. 603–612.

[6]Peracchio, A. A., and Proscia, W. M., "Nonlinear Heat Release/Acoustic Model for Thermoacoustic Instability in Lean Premixed Combustors," *Journal of Engineering for Gas Turbines and Power*, Vol. 121, No. 3, 1999, pp. 415–421.

[7]Brookes, S. J., Cant, R. S., Dupere, I. D., and Dowling, A. P., "Computational Modeling of Self-Excited Combustion Instabilities," American Society of Mechanical Engineers, Paper 2000-GT-0104, May 2000.

[8]Kruger, U., Huren, J., Hoffinan, S., Krebs, W., and Bohn. D., "Prediction of Thermoacoustic Instabilities with Focus on the Dynamic Flame Behavior for the 3A-Series Gas Turbine of Siemens KWU," American Society of Mechanical Engineers, Paper 99-GT-11, June 1999.

[9]Harrje, D. T., and Reardon, F. H., "Liquid Propellant Rocket Combustion Instability," NASA SP-194, 1971.

[10]Arana, C. A., Sekar, B., and Mawid, M. A., "Determination of Thermoacoustic Response in a Demonstrator Gas Turbine Engine," *Journal of Engineering for Gas Turbines and Power*, Vol. 124, No. 1, 2000, pp. 46–57.

[11]Fleifil, M., Annaswamy, A. M., Ghoneim, Z. A., and Ghoniem, A. F., "Response of a Laminar Flame to Flow Oscillations: A Kinematic Model and Thermoacoustic Instability Results," *Combustion and Flame*, Vol. 106, No. 4, 1996, pp. 487–510.

[12]Steele, R. C., Cowell, L. H., Cannon, S. M., and Smith, C. E., "Passive Control of Combustion Instability in Lean Premixed Combustors," *Journal of Engineering for Gas Turbines and Power*, Vol. 122, No. 3, 2000, pp. 412–419.

[13]Richards, G. A., and Janus, M. C., "Characterization of Oscillations During Premix Gas Turbine Combustion," *Journal of Engineering for Gas Turbines and Power*, Vol. 120, No. 2, 1998, pp. 294–302.

[14]Keller, J. J., "Thermoacoustic Oscillations in Combustion Chambers of Gas Turbines," *AIAA Journal*, Vol. 33, No. 12, 1995, pp. 2280–2287.

[15]Lieuwen, T., and Zinn, B. T., "The Role of Equivalence Ratio Oscillations in Driving Combustion Instabilities in Low NOx Gas Turbines," *Proceedings of the Combustion Institute,* Vol. 27, 1998, pp. 1809–1816.

[16]Lee, J. G., Kim, K., and Santavicca, D. A., "Measurement of Equivalence Ratio Fluctuation and Its Effect on Heat Release During Unstable Combustion," *Proceedings of the Combustion Institute*, Vol. 28, 2000, pp. 415–421.

[17]Mongia, R. K., Tomita, E., Hsu, F. K., Talbot, L., and Dibble, R. W., "Use of an Optical Probe for Time-Resolved in situ Measurement of Local Air-to-Fuel Ratio and Extent of Fuel Mixing with Applications to Low NOx Emission in Premixed Gas Turbines," *Proceedings of the Combustion Institute*, Vol. 26, 1996, pp. 2749–2755.

[18]Schadow, K. C., and Gutmark, E., "Combustion Instabilities Related to Vortex Shedding in Dump Combustors and Their Passive Control," *Progress in Energy and Combustion Science*, Vol. 18, No. 2, 1992, pp. 117–132.

[19]Smith, D. A., "An Experimental Study of Acoustically Excited, Vortex Driven Combustion Instability Within a Rearward Facing Step Combustor," Ph.D. Dissertation, Dept. of Mechanical Engineering, California Inst. of Technology, Pasadena, 1985.

[20]Sterling, J. D., and Zukoski, E. E., "Longitudinal Mode Combustion Instabilities in a Dump Combustor," AIAA Paper 87-0220, Jan. 1987.

[21]Gutmark, E., Schadow, K. C., Sivasegaram, S., and Whitelaw, J. H., "Interaction Between Fluid-Dynamic and Acoustic Instabilities in Combusting Flows Within Ducts," *Combustion Science and Technology*, Vol. 79, No. 1–3, 1991, pp. 161–166.

[22]Poinsot, T. J., Trouve, A. C., Veynante, D. P., Candel, S. M., and Esposito, E. J., "Vortex-Driven Acoustically Coupled Combustion Instabilities," *Journal of Fluid Mechanics*, Vol. 177, 1987, pp. 265–292.

[23]Langhorne, P. J., "Reheat Buzz: An Acoustically Coupled Combustion Instability, Part 1, Experiment," *Journal of Fluid Mechanics*, Vol. 193, 1988, pp. 417–443.

[24]Yu, K. H., Trouve, A., and Daily, J. W., "Low-Frequency Pressure Oscillations in a Model Ramjet Combustor," *Journal of Fluid Mechanics*, Vol. 232, 1991, pp. 47–72.

[25]Schuermans, B. H., and Polifke, W., "Modeling Transfer Matrices of Premixed Flames and Comparison with Experimental Results," American Society of Mechanical Engineers, Paper 99-GT-132, June 1999.

[26]Kendrick, D. W., Anderson, T. J., Sowa, W. A., and Snyder, T. S., "Acoustic Sensitivities of Lean-Premixed Fuel Injectors in a Single Nozzle Rig," *Journal of Engineering for Gas Turbines and Power*, Vol. 121, No. 3,1999, pp. 429–436.

[27]Paschereit, C. O., Flohr, P., Knopfel, H., Geng, W., Steinbach, C., Stuber, P., Bengtsson, K., and Gutmark, E., "Combustion Control by Extended EV Burner Fuel Lance," American Society of Mechanical Engineers, Paper GT-2002-30462, June 2002.

[28]Munjal, M. L., *Acoustics of Ducts and Mufflers*, Wiley, New York, 1987.

[29]Fannin, C. A., Baumann, W. T., Saunders, W. R., Richards, G. A., and Straub, D. L., "Thermoacoustic Stability Analysis for Mutli-Port Fuel Injection in a Lean Premixed Combustor," AIAA Paper 2000-0711, Jan. 2000.

[30]Phillips, C. L., and Harbor, R. D., *Feedback Control Systems*, 4th ed., Prentice–Hall, Upper Saddle River, NJ, 2000.

[31]Blackshear, P. L., "Driving Standing Waves by Heat Addition," *Proceedings of the Combustion Institute*, Vol. 4, 1953, pp. 553–556.

[32]Merk, H. J., "An Analysis of Unstable Combustion of Premixed Gases," *Proceedings of the Combustion Institute*, Vol. 6, 1956, pp. 501–512.

[33]Becker, R., and Gunther, R., "The Transfer Function of Premixed Turbulent Jet Flames," *Proceedings of the Combustion Institute*, ASHRAE, Vol. 13, 1971, pp. 517–526.

[34]Baade, P. K., "Design Criteria and Models for Preventing Combustion Oscillations," *Transactions of the ASHRAE 84 (Part 1)*, 1978.

[35]Mugridge, B. D., "Combustion Driven Oscillations," *Journal of Sound and Vibration*, Vol. 70, No. 3, 1980, pp. 437–452.

[36]Matsui, Y., "An Experimental Study on Pyro-Acoustic Amplification of Premixed Laminar Flames," *Combustion and Flame*, Vol. 43, 1981, pp. 199–209.

[37]Ducruix, S., Durox, D., and Candel, S., "Theoretical and Experimental Determination of the Transfer Function of a Laminar Premixed Flame," *Proceedings of the Combustion Institute*, Vol. 28, 2000, pp. 765–773.

[38]Hadvig, S., "Combustion Instability: System Analysis," *Journal of the Institute of Fuel*, Vol. 44, 1971, pp. 550–558.

[39]Hegde, U. G., Reuter, D., Daniel, B. R., and Zinn, B. T., "Flame Driving of Longitudinal Instabilities in Dump Type Ramjet Combustors," *Combustion Science and Technology*, Vol. 55, No. 1–3, 1987, pp. 125–138.

[40]Fieler, C. E., and Heidmann, M. F., "Dynamic Response of Gaseous Hydrogen Flow Systems and Its Application to High-Frequency Combustion Instability," NASA TN D-4040, 1967.

[41]Putnam, A. A., *Combustion Driven Oscillations in Industry*, Elsevier, New York, 1971.

[42]Janardan, B. A., Daniel, B. R., and Zinn, B. T., "Driving of Combustion Oscillations by Gaseous Propellant Injectors," *Proceedings of the Combustion Institute*, Vol. 17, 1977, pp. 1353–1361.

[43]Lieuwen, T., and Zinn, B. T., "Theoretical Investigation of Premixed Combustion Instability Mechanisms," AIAA Paper 98-0641, Jan. 1998.

[44]Richards, G. A., Straub, D. L., and Robey, E. H., "Dynamic Response of A Premix Fuel Injector," American Society of Technical Engineers, Paper 2001-GT-036, June 2001.

[45]Scarinci, T., and Freeman, C., "The Propagation of a Fuel-Air Ratio Disturbance in a Simple Premixer and Its Influence on Pressure Wave Amplification," American Society of Mechanical Engineers, Paper 2000-GT-0106, May 2000.

[46]Sattlelmayer, T., "Influence of the Combustor Aerodynamics on Combustion Instabilities From Equivalence Ratio Fluctuations," American Society of Mechanical Engineers, Paper 2000-GT-0082, May 2000.

[47]Mongia, R., Dibble, R., and Lovett, J., "Measurement of Air-Fuel Ratio Fluctuations Caused by Combustor Driven Oscillations," American Society of Mechanical Engineers, Paper 98-GT-304, June 1998.

[48]Anderson, T. J., Sowa, W. A., and Morford, S. A., "Dynamic Flame Structure in a Low NOx Premix Combustor," American Society of Mechanical Engineers, Paper 98-GT-568, June 1998.

[49]Paschereit, C. O., Polifke, W., Schuermns, B., and Mattson, O., "Measurement of Transfer Matrices and Source Terms of Premixed Flames," *Journal of Engineering for Gas Turbines and Power*, Vol. 124, No. 2, 2002, pp. 239–247.

[50]Lawn, C. J., "Thermo-Acoustic Frequency Selection by Swirled Premixed Flames," *Proceedings of the Combustion Institute*, Vol. 28, 2000, pp. 823–830.

[51]Krebs, W., Hoffman, S., Prade, B., Lohrmann, M., and Buchner, H., "Thermoacoustic Flame Response of Swirl-Stabilized Flames," American Society of Mechanical Engineers, Paper GT-2002-30065, June 2002.

[52]Khanna, V. K., "A Study of the Dynamics of Laminar and Turbulent Fully and Partially Premixed Flames," Ph.D. Dissertation, Dept. of Mechanical Engineering, Virginia Polytechnic Inst. and State Univ., Blacksburg, VA, 2001.

[53]Khanna, V., Vandsburger, U., Saunders, W. R., and Baumann, W. T., "Dynamic Analysis of Swirl Stabilized Turbulent Gaseous Flame," American Society of Mechanical Engineers, Paper GT-2002-30061, June 2002.

[54]Bohn, D., Deutsch, G., and Kruger, U., "Numerical Prediction of the Dynamic Behavior of Turbulent Diffusion Flames," *Journal of Engineering for Gas Turbines and Power*, Vol. 120, No. 4, 1998, pp. 713–720.

[55]Bohn, D., Li, Y., Matouschek, G., and Kruger, W., "Numerical Prediction of the Dynamic Behavior of Premixed Flames Using Systematically Reduced Multi-Step Reaction Mechanisms," American Society of Mechanical Engineers, Paper 97-GT-265, June 1997.

[56]Kruger, U., Hoffman, S., Krebs, W., Judith, H., Bohn, D., and Matouschek, G., "Influence of Turbulence on the Dynamic Behavior of Premixed Flames," American Society of Mechanical Engineers, Paper 98-GT-323, June 1998.

[57]Smith, C. E., and Leonard, A. D., "CFD Modeling of Combustion Instability in Premixed Axisymmetric Combustors," American Society of Mechanical Engineers, Paper 97-GT-305, June 1997.

[58]Zhu, M., Dowling, A. P., and Bray, K. N. C., "Flame Transfer Calculations for Combustion Oscillations," American Society of Mechanical Engineers, Paper 2001-GT-0374, June 2001.

[59]Walz, G., Krebs, W., Hoffmann, S., and Judith, H., "Detailed Analysis of the Acoustic Mode Shapes of an Annular Combustion Chamber," American Society of Mechanical Engineers, Paper 99-GT-113, June 1999.

[60]Cronemyr, P. J. M., Hulme, C. J., and Troger, C., "Coupled Acoustic-Structure Analysis of an Annular DLE Combustor," American Society of Mechanical Engineers, Paper 98-GT-502, June 1998.

[61]Pankiewitz, C., and Sattelmayer, T., "Time Domain Simulation of Combustion Instabilities in Annular Combustor," American Society of Mechanical Engineers, Paper GT-2002-30063, June 2002.

[62]Evesque, S., and Polifke, W., "Low-Order Acoustic Modeling for Annular Combustors: Validation and Inclusion of Modal Coupling," American Society of Mechanical Engineers, Paper GT-2002-30064, June 2002.

[63]Krebs, W., Walz, G., Flohr, P., and Hoffmann, S., "Modal Analysis of Annular Combustors: Effect of Burner Impedance," American Society of Mechanical Engineers, Paper 2001-GT-0042, June 2001.

[64]Straub, D. L., and Richards, G. A., "Effect of Fuel Nozzle Configuration on Premix Combustion Dynamics," American Society of Mechanical Engineers, Paper 98-GT-492, June 1998.

[65]Hermsmeyer, H., Prade, B., Gruschka, U., Schmitz, U., Hoffmann, S., and Krebs, W., "V64.3A Gas Turbine Natural Gas Burner Development," American Society of Mechanical Engineers, Paper GT-2002-30106, June 2002.

[66]Lieuwen, T., Torres, H., Johnson, C., and Zinn, B. T., "A Mechanism of Combustion Instability in Lean Premixed Gas Turbine Combustors," *Journal of Engineering for Gas Turbines and Power*, Vol. 123, No. 1, 2001, pp. 182–189.

[67]Lovett, J. A., and Uznanski, K. T., "Prediction of Combustion Dynamics in a Staged Premixed Combustor," American Society of Mechanical Engineers, Paper GT-2002-30646, June 2002.

[68]Berenbrink, P., and Hoffmann, S. "Suppression of Dynamics Combustion Instabilities by Passive and Active Means," American Society of Mechanical Engineers, Paper 2000-GT-0079, May 2000.

[69]Richards, G. A., Straub, D. L., and Robey, E. H. "Control of Combustion Dynamics Using Fuel System Impedance," American Society of Mechanical Engineers, Paper GT-2003-38521, June 2003.

[70]Lee, J. G., Kim, K., and Santavicca, D. A., "A Study of the Role of Equivalence Ratio Fluctuations During Unstable Combustion in a Lean Premixed Combustor," AIAA Paper 2002-4015, July 2002.

[71]Lovett, J. A. , "Bluffbody Flameholders for Low-Emission Gas Turbine Combustors", U.S. Patent 5, 471,840, Dec. 1995.

[72]Straub, D. L., Richards, G. A., Baumann, W. T., and Saunders, W. R., "Measurement of Dynamics Flame Response in a Lean Premixed Single-Can Combustor," American Society of Mechanical Engineers, Paper 2001-GT-0038, June 2001.

[73]Laudien, E., Pongratz, R., Pierro, R., and Preclik, D., "Experimental Procedures Aiding the Design of Acoustic Cavities," *Liquid Rocket Engine Combustion Instability*, Progress in Astronautics and Aeronautics, edited by V. Yang and W. E. Anderson, Vol. 169, AIAA, Washington, DC, 1995, pp. 377–399.

[74]Lewis, G. D., and Garrison, G. D., "The Role of Acoustic Absorbers in Preventing Combustion Instability," AIAA Paper 71-699, June 1971.

[75]Gysling, D. L., Copeland, G. S., McCormick, D. C., and Proscia, W. M., "Combustion System Damping Augmentation with Helmholtz Resonators," American Society of Mechanical Engineers, Paper 98-GT-268, June 1998.

[76]Bellucci, V., Paschereit, C. O., Flohr, P., and Magni, F., "On the Use of Helmholtz Resonators for Damping Acoustic Pulsations in Industrial Gas Turbines," American Society of Mechanical Engineers, Paper 2001-0039, June 2001.

[77]Mitchell, C. E., "Analytical Models for Combustion Instability in Liquid Rocket Engine Combustion Instability," *Liquid Rocket Engine Combustion Instability*, Progress in Astronautics and Aeronautics, edited by V. Yang and W. E. Anderson, Vol. 169, AIAA, Washington, DC, 1995, pp. 403–430.

[78]DeBiasi, V., "Gasification on Track to Turn Problem Fuels into Electricity and Power," *Gas Turbine World*, Nov.–Dec. 1999, pp. 12–20.